

# Bayesian Variable Selection for Non-Gaussian Responses: A Marginally Calibrated Copula Approach

Nadja Klein<sup>1</sup> and Michael Stanley Smith<sup>2,\*</sup>

<sup>1</sup>Humboldt Universität zu Berlin

<sup>2</sup>Melbourne Business School, University of Melbourne

\* Michael Stanley Smith is Professor of Management (Econometrics) at Melbourne Business School, University of Melbourne. Nadja Klein is Assistant Professor of Applied Statistics, at Humboldt-Universität zu Berlin. Correspondence should be directed to Michael Stanley Smith at 200 Leicester Street, Carlton, VIC 3053, Australia (mike.smith@mbs.edu). Nadja Klein gratefully acknowledges funding from the Alexander von Humboldt foundation.

# Bayesian Variable Selection for Non-Gaussian Responses: A Marginally-Calibrated Copula Approach

## Abstract

We propose a new highly flexible and tractable Bayesian approach to undertake variable selection in non-Gaussian regression models. It uses a copula decomposition for the vector of observations on the dependent variable. This allows the marginal distribution of the dependent variable to be calibrated accurately using a nonparametric or other estimator. The family of copulas employed are ‘implicit copulas’ that are constructed from existing hierarchical Bayesian models used for variable selection, and we establish some of their properties. Even though the copulas are high-dimensional, they can be estimated efficiently and quickly using Monte Carlo methods. A simulation study shows that when the responses are non-Gaussian the approach selects variables more accurately than contemporary benchmarks. A marketing example illustrates that accounting for even mild deviations from normality can lead to a substantial improvement. To illustrate the full potential of our approach we extend it to spatial variable selection for fMRI data. It allows for voxel-specific marginal calibration of the magnetic resonance signal at over 6,000 voxels, leading to a considerable increase in the quality of the activation maps.

**Keywords:** fMRI; Inversion copulas; Mixtures of hyper-g priors; Spatial Bayesian variable selection.

# 1 Introduction

Bayesian approaches to selecting covariates in regression models are well established; see Clyde and George (2004); O’Hara and Sillanpää (2009) and Bottolo and Richardson (2010) for overviews. However, most work remains focused on Gaussian regression models, and extensions to the non-Gaussian case are still limited. In particular, the importance of distributional calibration (Gneiting et al., 2007) in Bayesian variable (ie. covariate) selection remains unexplored. We address this question here by proposing a new Bayesian approach to covariate selection that is based on a copula decomposition for the vector of observations of length  $n$  on the dependent variable. The impact of the covariates on the dependent variable is captured by the copula function only. This separates the task of selecting covariates from that of modeling the marginal distribution of the dependent variable; the latter of which can then be calibrated accurately—either parametrically or non-parametrically—regardless of its distributional form. For the copula function we propose a new family of ‘implicit copulas’, which are constructed from existing Bayesian hierarchical regression models used for selecting covariates. The result is a very general and tractable approach that extends Bayesian variable selection methodology to data that have an arbitrary marginal distribution. Our aim is to show that by doing so, accurate marginal calibration increases the precision of covariate selection, and also the accuracy of the predictive distribution of the dependent variable.

Lower dimensional copulas are often used to capture dependence between multiple variables (Nelsen, 2006; Joe, 2015). We stress that the copula is used here in a very different way to capture the dependence between multiple observations on just one dependent variable. The specification of this  $n$ -dimensional copula function is the key ingredient of our method. Few existing copulas can be used in such high dimensions, although implicit copulas constructed by the inversion of a parametric distribution (Nelsen, 2006, Sec.3.1) can. To construct a copula family we consider a Gaussian linear model for  $n$  observations on a second dependent variable, which we label a ‘pseudo-response’ because it is not observed directly. Gaussian spike-and-slab priors (Smith and Kohn, 1996; George and McCulloch, 1997) with selection indicator variables  $\gamma$  are employed for the coefficients, which are integrated out to obtain the distribution of the pseudo-response vector conditional on the covariates and  $\gamma$ . This is a Gaussian distribution, and its implicit copula is the popular Gaussian copula func-

tion (Song, 2000) with a parameter matrix that is a function of both the covariate values and  $\gamma$ . Finally, to obtain our copula family we mix this Gaussian copula over the scaling factor  $g$  of the non-zero coefficients with respect to the different hyper-priors suggested by Liang et al. (2008). The resulting implicit copulas are not Gaussian copulas, and we derive some of their properties.

Because of its high dimension, it is difficult to evaluate the implicit copula directly. However, we show how to construct a Markov chain Monte Carlo (MCMC) sampler to undertake stochastic search variable selection (George and McCulloch, 1993), where the scaling factor  $g$  is generated using the Hamiltonian Monte Carlo (HMC) method of Hoffman and Gelman (2014). Careful use of matrix identities for the computations makes application of the method to high dimensions practical. A simulation study and a real marketing data example, with  $p = 20$  and  $p = 252$  covariates respectively, compare our approach to Gaussian Bayesian variable selection and the high performing method of Rossell and Rubio (2018). They show that accurate marginal calibration can result in more precise covariate selection, along with more accurate predictive densities for the dependent variable.

To illustrate the generality of our approach, we extend it to spatial variable selection for functional magnetic resonance imaging (fMRI). In these studies a large vector of binary indicators signifies which voxels in a partition of the brain are active. We follow Smith and Fahrmeir (2007), Li and Zhang (2010) and Goldsmith et al. (2014) and use an Ising density as a prior to smooth these spatially, but employ our implicit copula model to allow for voxel-wise marginal calibration of the magnetic resonance (MR) signal. The neuroimaging literature suggests that accounting for deviations from normality in the MR signal is important to obtain accurate activation maps (Eklund et al., 2017). Application of our approach to data from a visual experiment with 6192 voxels shows this to be true here, and also produces much more accurate voxel-wise predictive distributions for the MR signal, as measured by the logarithmic scores.

A number of other approaches allow Bayesian variable selection for non-Gaussian continuous-valued data. These include conditionally Gaussian models, where the disturbances follow a mixture of normals and/or data transformations of the dependent variable are considered (Smith and Kohn, 1996; Gottardo and Raftery, 2009; Wang et al., 2017; Ranciati et al., 2019). Rossell and Rubio (2018) propose a Bayesian variable selection approach that allows for skewness and thicker tails compared to the Gaussian distribution but cover only two-

piece errors applied to the Gaussian and Laplace distributions. Chung and Dunson (2009); Kundu and Dunson (2014) propose non-parametric models where the mean and shape learn the effect of covariates, but assume symmetric residuals. Yu et al. (2013) propose variable selection in Bayesian quantile regression using a latent scale augmentation of the asymmetric Laplace errors and Yan and Kottas (2017) extend Azzalini’s skew normal to Laplace errors in Bayesian quantile regression with LASSO penalties. However, none of these approaches fits our copula framework or ensures accurate calibration of the marginal distribution of the response. Sharma and Das (2018) recently proposed an alternative class of non-conjugate priors for regression coefficients based on copulas; however this is very different from our use of copulas to build a non-Gaussian regression model here. Last, Kraus and Czado (2017) use a D-vine copula to capture flexibly dependence between covariates and response in a regression model, also allowing for accurate marginal calibration for the response. However, this approach uses a copula in a very different way than that suggested here, and does not generalize existing Bayesian variable selection schemes. For example, it could not be employed to undertake spatial variable selection for fMRI as considered here.

The rest of this paper is structured as follows. Section 2 outlines our approach, including derivation of the implicit copula and some of its properties. Section 3 outlines how to compute Bayesian inference using stochastic search, along with the predictive densities of the dependent variable and Bayes factors for model comparison. Section 4 contains the simulation study, and Section 5 the analysis of the marketing data. Section 6 extends the approach to spatial variable selection for fMRI data, and Section 7 concludes.

## 2 Variable Selection in Regression using Copulas

### 2.1 Marginally calibrated variable selection

Consider a vector  $\mathbf{Y} = (Y_1, \dots, Y_n)'$  of  $n$  realisations on a continuous dependent variable, along with an  $n \times p$  design matrix  $X$  for  $p$  regression covariates. Bayesian approaches to variable selection usually proceed by introducing a vector of binary indicator variables  $\boldsymbol{\gamma} = (\gamma_1, \dots, \gamma_p)'$ , such that the  $i$ th covariate is included in the regression if  $\gamma_i = 1$ , and excluded if  $\gamma_i = 0$ . When the dependent variable is non-Gaussian, the most common approach is to consider non-Gaussian distributions for the disturbance to a linear model; for example, see Chung and Dunson (2009); Rossell and Rubio (2018) and references therein. Thus, either

a parametric or non-parametric non-Gaussian distribution is selected for  $Y_i$ , conditional on  $X$  and  $\gamma$ . In this paper we suggest an alternative approach based on copulas that allows the marginal distribution of  $Y_i$ , unconditional on  $X$  and  $\gamma$ , to be selected instead.

To define our model, let  $Y_i|X, \gamma$  have distribution and density functions  $F_{Y_i}(y_i|X, \gamma)$  and  $p_{Y_i}(y_i|X, \gamma)$ , respectively. Then the copula representation (Sklar, 1959) of the joint density of  $\mathbf{Y}|X, \gamma$  is  $p(\mathbf{y}|X, \gamma) = c^\dagger(\mathbf{u}|X, \gamma) \prod_{i=1}^n p_{Y_i}(y_i|X, \gamma)$ , where  $\mathbf{y} = (y_1, \dots, y_n)'$ ,  $\mathbf{u} = (u_1, \dots, u_n)'$ ,  $u_i = F_{Y_i}(y_i|X, \gamma)$  and  $c^\dagger$  is a copula density. However, in general  $c^\dagger$  and  $F_{Y_i}(y_i|X, \gamma)$  are both unknown, so that in copula modelling it is typical to select forms for both. In this paper we model the joint density as

$$p(\mathbf{y}|X, \gamma) = c_{\text{BVS}}(\mathbf{u}|X, \gamma) \prod_{i=1}^n p_Y(y_i). \quad (1)$$

Above, the distribution of  $Y_i$  is assumed to be *marginally* invariant with respect to  $X$  and  $\gamma$ , with density  $p_{Y_i} = p_Y$  and distribution function  $F_{Y_i} = F_Y$  for all  $i$ . Instead, the impact of the covariate values  $X$  and model indicators  $\gamma$  on  $\mathbf{Y}$  *jointly* is captured through the copula with density  $c_{\text{BVS}}$ , which is a function of  $X$  and  $\gamma$ . For this we use the copula proposed in Section 2.2 below.

A major advantage of employing Eq. (1) is that it separates the modeling of the marginal distribution  $F_Y$  of the data, from the task of selecting the covariates. Therefore,  $F_Y$  can be calibrated accurately, and we chose to model it non-parametrically in our work. Variable selection is based on the posterior distribution of  $\gamma$ , which is given by

$$p(\gamma|X, \mathbf{y}) \propto p(\mathbf{y}|X, \gamma)p(\gamma) \propto c_{\text{BVS}}(\mathbf{u}|X, \gamma)p(\gamma), \quad (2)$$

with model prior  $p(\gamma)$  and  $u_i = F_Y(y_i)$ . A major aim of this paper is to show that adopting Eq. (1) with our proposed copula provides a very general, but tractable, approach to undertaking variable selection and model averaging for non-Gaussian regression data.

We make two remarks concerning the appropriateness of the decomposition at Eq. (1). First, regression models are usually specified conditional on parameters for the mean, variance and possibly other moments. In contrast, the expressions above are unconditional on such parameters. We show later in Section 2.4 that when also conditioning on additional model parameters, the distribution of  $Y_i$  is a function of the covariates, as is expected in a regression model. Second, the assumption that density  $p_Y$  is not a function of  $X$  is consistent with the standard Gaussian linear regression model. For example, when a proper g-prior is used for the regression coefficients, the margin of  $Y_i$  with the coefficients and error variance

integrated out is asymptotically independent of  $X$ ; see Appendix A for a proof.

Last, consider a new realization  $Y_{n+1}$  of the dependent variable, with a  $p \times 1$  vector of observed covariate values  $\mathbf{x}_{n+1}$ . To see how it is directly affected by the covariates and indicators, let  $X^+ = [X'|\mathbf{x}_{n+1}]'$  and  $\mathbf{u}^+ = (\mathbf{u}', F_Y(y_{n+1}))'$ , then from Eq. (1),  $Y_{n+1}$  has predictive density conditional on  $\gamma$ :

$$p(y_{n+1}|X^+, \gamma, \mathbf{y}) = \frac{p(y_{n+1}, \mathbf{y}|X^+, \gamma)}{p(\mathbf{y}|X, \gamma)} = \frac{c_{\text{BVS}}(\mathbf{u}^+|X^+, \gamma)}{c_{\text{BVS}}(\mathbf{u}|X, \gamma)} p_Y(y_{n+1}). \quad (3)$$

This is a function of the observations on all the covariates, and the indicator variables  $\gamma$ . Moreover, marginalizing over the posterior of  $\gamma$  gives the posterior predictive density for  $Y_{n+1}|X^+, \mathbf{y}$  as

$$p(y_{n+1}|X^+, \mathbf{y}) = \sum_{\gamma} p(y_{n+1}|X^+, \gamma, \mathbf{y}) p(\gamma|X, \mathbf{y}). \quad (4)$$

Eq. (4) forms the basis of the model average predictive distribution of  $Y_{n+1}$  from the copula model, and we show how to evaluate it efficiently in Section 3.2.2.

## 2.2 Variable selection copula

Key to our approach is the specification of our proposed copula function  $C_{\text{BVS}}$  with density  $c_{\text{BVS}} = \frac{\partial}{\partial \mathbf{u}} C_{\text{BVS}}$ . To derive these, we consider the linear model

$$\tilde{\mathbf{Z}} = X_{\gamma} \boldsymbol{\beta}_{\gamma} + \boldsymbol{\varepsilon}, \quad (5)$$

where  $\tilde{\mathbf{Z}} = (\tilde{Z}_1, \dots, \tilde{Z}_n)'$ ,  $X_{\gamma}$  is an  $n \times q_{\gamma}$  sub-matrix of  $X$  that comprises the columns of  $X$  where  $\gamma_i = 1$ ,  $\boldsymbol{\beta}_{\gamma}$  are the corresponding regression coefficients, and  $\boldsymbol{\varepsilon} \sim N(\mathbf{0}, \sigma^2 I)$ . We refer to  $\tilde{\mathbf{Z}}$  as a vector of observations on a ‘pseudo-response’, because it is not observed directly in our model. Following Smith and Kohn (1996); George and McCulloch (1997); Liang et al. (2008) and many others, the conjugate g-prior of Zellner (1986)

$$\boldsymbol{\beta}_{\gamma}|X, \sigma^2, \gamma, g \sim N(0, g\sigma^2(X_{\gamma}'X_{\gamma})^{-1}), \quad g > 0, \quad (6)$$

is used for the non-zero coefficients. The use of this prior has been much discussed in the context of a linear model; for example, see Clyde and George (2004) or Liang et al. (2008). Its conjugacy and scaling prove attractive features for constructing the variable selection copula.

To construct the variable selection copula, we first extract the ‘implicit’ copula of the joint distribution of  $\tilde{\mathbf{Z}}$  conditional on  $X, \gamma, g, \sigma^2$ , but with  $\boldsymbol{\beta}_{\gamma}$  integrated out. Implicit copulas—also called ‘inversion’ copulas—are obtained by inverting the usual expression of

Sklar's theorem; see Nelsen (2006, Sec. 3.1). Here, we construct it from the distribution  $\tilde{\mathbf{Z}}|X, \boldsymbol{\gamma}, g, \sigma^2 \sim N(\mathbf{0}; \Omega)$ , where

$$\Omega = \sigma^2 \left( I - \frac{g}{1+g} X_\gamma (X_\gamma' X_\gamma)^{-1} X_\gamma' \right)^{-1} = \sigma^2 (I + g X_\gamma (X_\gamma' X_\gamma)^{-1} X_\gamma'),$$

which follows from integrating out  $\boldsymbol{\beta}_\gamma$  as a normal, and applying the Woodbury formula. The implicit copula of a normal distribution is the Gaussian copula (Song, 2000), with parameter matrix equal to the correlation of the distribution. To derive this matrix we standardize by the marginal variances

$$\text{Var}(\tilde{Z}_i|X, \boldsymbol{\gamma}, g, \sigma^2) = \sigma^2 (1 + g \mathbf{x}_{\gamma,i}' (X_\gamma' X_\gamma)^{-1} \mathbf{x}_{\gamma,i}) \equiv \sigma^2 s_i^{-2}, \text{ for } i = 1, \dots, n,$$

where  $\mathbf{x}_{\gamma,i}'$  is the  $i$ th row of  $X_\gamma$ . If  $S_\gamma \equiv S(X, \boldsymbol{\gamma}, g) = \text{diag}(s_1, \dots, s_n)$ , then the correlation matrix is

$$R \equiv R(X, \boldsymbol{\gamma}, g) = \frac{1}{\sigma^2} S_\gamma \Omega S_\gamma = S_\gamma (I + g X_\gamma (X_\gamma' X_\gamma)^{-1} X_\gamma') S_\gamma. \quad (7)$$

Thus, the implicit copula of the distribution of  $\tilde{\mathbf{Z}}$  (conditional on  $X, \boldsymbol{\gamma}, g, \sigma^2$ ) is the Gaussian copula function

$$C_{\text{Ga}}(\mathbf{u}; R) = \Phi(\Phi_1^{-1}(u_1), \dots, \Phi_1^{-1}(u_n); \mathbf{0}, R),$$

with density

$$c_{\text{Ga}}(\mathbf{u}; R) = |R|^{-1/2} \exp\left(-\frac{1}{2} \mathbf{z}' (R^{-1} - I) \mathbf{z}\right),$$

where  $\Phi(\cdot; \mathbf{0}, R)$  and  $\Phi_1(\cdot)$  are  $N(\mathbf{0}, R)$  and  $N(0, 1)$  distribution functions, respectively, and  $\mathbf{z} = (\Phi^{-1}(u_1), \dots, \Phi^{-1}(u_n))'$  (Song, 2000). Note that the location and scale of  $\tilde{\mathbf{Z}}$  are unidentified in its copula, with  $\sigma^2$  not featuring in the copula parameter matrix  $R$ . Therefore, without loss of generality, throughout the paper we set  $\sigma^2 = 1$  and do not include an intercept in  $X$ .<sup>1</sup>

Finally, we mix over  $g$  with respect to its prior  $p(g)$  to obtain the variable selection copula as a continuous mixture of Gaussian copulas, as defined below.

**Definition 1.** *Let  $C_{\text{Ga}}$  and  $c_{\text{Ga}}$  be the Gaussian copula function and density, respectively. Then if  $\tilde{\mathbf{Z}}$  follows the linear model at Eq. (5), with the  $g$ -prior for  $\boldsymbol{\beta}_\gamma$  at Eq. (6), and  $p(g)$  is a proper density for  $g > 0$ , then we call*

$$C_{\text{BVS}}(\mathbf{u}|X, \boldsymbol{\gamma}) = \int C_{\text{Ga}}(\mathbf{u}; R(X, \boldsymbol{\gamma}, g)) p(g) dg$$

---

<sup>1</sup>We stress here that this does not mean the observational data  $Y_i$  has zero mean or fixed scale. Instead, these are captured through the margin  $F_Y$  in Eq. (1).



a variable selection copula, with density function

$$c_{BVS}(\mathbf{u}|X, \boldsymbol{\gamma}) = \int c_{Ga}(\mathbf{u}; R(X, \boldsymbol{\gamma}, g))p(g)dg.$$

Moreover, it is straightforward to show the following Corollary:

**Corollary 1.** *The function  $C_{BVS}(\mathbf{u}|X, \boldsymbol{\gamma})$  is a well-defined copula function.*

We consider the three priors discussed by Liang et al. (2008) for  $g$ , along with a point mass, as listed below:

- (a) *Hyper-g prior:* with density  $p(g) = \frac{a-2}{2}(1+g)^{-a/2}$ , which is proper for  $a > 2$  and  $a = 2$  corresponds to both the Jeffrey's and reference prior. Note that this prior implies a Beta prior on the shrinkage factor  $g/(1+g) \sim \text{Beta}(1, 0.5a - 1)$  with mean  $2/a$ , and we set  $a = 4$ , leading to a uniform prior on this shrinkage factor.
- (b) *Hyper-g/n prior:* with density  $p(g) = \frac{a-2}{2n}(1+g/n)^{-a/2}$ . This prior is motivated by the lack of consistency of the hyper-g prior in the linear model.
- (c) *Zellner-Siow prior:* with density  $p(g) = \frac{\sqrt{n/2}}{\Gamma(1/2)}c^{-3/2} \exp(-n/(2g))$ . This prior is less popular for a linear model because the marginal distributions of the dependent variable are not of closed form. However, the margin if  $Y_i$  is selected directly in the copula model at Eq. (1), so this is not an issue when constructing a variable selection copula.
- (d) *Point mass prior:* We also consider fixing  $g = 100$  (ie. a point mass) for comparison.

While computing the integral over  $g$  in Defn. 1 is possible using numerical methods, in general it is difficult to evaluate  $C_{BVS}$  or  $c_{BVS}$  directly because  $R(X, \boldsymbol{\gamma}, g)$  is an  $n$ -dimensional matrix. Instead, when computing inference we generate  $g$  as part of a Markov chain Monte Carlo (MCMC) scheme, as discussed in Section 3.

Last, for  $\boldsymbol{\gamma}$  we use the mass function  $p(\boldsymbol{\gamma}) = \text{Beta}(p - q_{\boldsymbol{\gamma}} + 1, q_{\boldsymbol{\gamma}} + 1)$ . This has been used extensively in the Bayesian selection literature because it accounts for the multiplicity of the  $2^p$  possible configurations of  $\boldsymbol{\gamma}$  (Scott and Berger, 2010). It implies a uniform prior distribution on  $p(q_{\boldsymbol{\gamma}}) = 1/(p + 1)$  and Bernoulli margins  $\Pr(\gamma_i = 1) = 1/2$ .

## 2.3 Copula properties

Here, we state some elementary properties of the copula  $C_{BVS}$ , with proofs given in the Online Appendix.

- (i) When  $\boldsymbol{\gamma} = \mathbf{0}$ , the variable selection copula is the independence copula (Nelsen, 2006,

p.11), with

$$C_{\text{BVS}}(\mathbf{u}|X, \mathbf{0}) = \prod_{i=1}^n u_i.$$

Below are some pairwise dependence metrics of the bivariate sub-copula of  $C_{\text{BVS}}$  in elements  $1 \leq i < j \leq n$ . This is defined as  $C_{\text{BVS}}^{ij}(u_i, u_j) = \int C_{\text{BVS}}(\mathbf{u}|X, \boldsymbol{\gamma}) d\mathbf{u}_{\setminus ij}$ , with  $\mathbf{u}_{\setminus ij}$  the sub-vector of  $\mathbf{u}$  without elements  $u_i, u_j$ .

(ii) For  $q \in (0, 1)$ , if  $(U_i, U_j) \sim C_{\text{BVS}}^{ij}$ , the lower and upper quantile dependence are

$$\begin{aligned} \lambda_{ij}^L(q|X, \boldsymbol{\gamma}) &\equiv \Pr(U_i < q|U_j < q) = \int \lambda_{1,ij}^L(q|X, \boldsymbol{\gamma}, g)p(g)dg, \text{ and} \\ \lambda_{ij}^U(q|X, \boldsymbol{\gamma}) &\equiv \Pr(U_i > q|U_j > q) = \int \lambda_{1,ij}^U(q|X, \boldsymbol{\gamma}, g)p(g)dg, \end{aligned}$$

where  $\lambda_{1,ij}^L$  and  $\lambda_{1,ij}^U$  are the lower and upper pairwise quantile dependences of a bivariate Gaussian copula with correlation parameter  $r_{ij}$  given by the  $(i, j)$ th element of  $R$  in Eq. (7).

(iii) The lower and upper extremal tail dependence

$$\lambda_{ij}^L = \lim_{q \downarrow 0} \lambda_{ij}^L(q|X, \boldsymbol{\gamma}) = 0, \text{ and } \lambda_{ij}^U = \lim_{q \uparrow 1} \lambda_{ij}^U(q|X, \boldsymbol{\gamma}) = 0.$$

(iv) Spearman's rho is

$$\rho_{ij}^S(X, \boldsymbol{\gamma}) = \frac{6}{\pi} \int \arcsin(r_{ij}/2)p(g)dg,$$

where  $r_{ij}$  is as defined above and is a function of  $X, \boldsymbol{\gamma}, g$ .

(v) Kendall's tau is

$$\tau_{ij}^K(X, \boldsymbol{\gamma}) = \frac{2}{\pi} \int \arcsin(r_{ij})p(g)dg.$$

The dependence metrics at properties (ii),(iv) and (iv) above are functions of the varying dimension parameters  $\boldsymbol{\gamma}$ , and also all the covariate values  $X$ , rather than just those corresponding to the  $i$ th and  $j$ th observations.

## 2.4 Margin of $Y_i$

In the copula decomposition at Eq. (1), it is assumed that  $Y_i$  is marginally independent of the covariates  $X$  and indicators  $\boldsymbol{\gamma}$ . However, to see how the covariate values are linked to the dependent variable, we derive the distribution of  $Y_i$  conditional on  $X, \boldsymbol{\gamma}$  and also on  $\boldsymbol{\beta}_\gamma$ . To do so, let  $Z_i = s_i \tilde{Z}_i$ , where as before  $\tilde{Z}_i$  is the pseudo-response with  $\sigma^2 = 1$ . From Eq. (5), this normalized pseudo-response has distribution  $Z_i|\mathbf{x}_i, \boldsymbol{\beta}_\gamma \sim N(s_i \mathbf{x}'_{\gamma,i} \boldsymbol{\beta}_\gamma, s_i^2)$ .

Because the copula model at Eq. (1) is an implicit copula model,  $Y_i$  can be expressed as the transformation  $Y_i = F_Y^{-1}(\Phi_1^{-1}(Z_i))$  of  $Z_i$ , with Jacobean  $\frac{p_Y(y_i)}{\phi_1(z_i)}$ . Then, the density

$$p(y_i|X, \boldsymbol{\beta}_\gamma, \boldsymbol{\gamma}) = p(z_i|X, \boldsymbol{\beta}_\gamma, \boldsymbol{\gamma}) \frac{p_Y(y_i)}{\phi_1(z_i)} = \frac{1}{s_i} \phi_1 \left( \frac{z_i - s_i \mathbf{x}_i' \boldsymbol{\beta}_\gamma}{s_i} \right) \frac{p_Y(y_i)}{\phi_1(z_i)}. \quad (8)$$

Thus, the distribution of  $Y_i$  is a function of  $\mathbf{x}_i$  when also conditioning on  $\boldsymbol{\beta}_\gamma$ .

### 3 Estimation and Inference

Estimation of the copula model at Eq. (1) requires estimation of both the marginal  $F_Y$  and parameters  $\boldsymbol{\gamma}$ . In the copula literature, it is popular to use two stage estimators—where  $F_Y$  is estimated first, followed by  $\boldsymbol{\gamma}$ —because they are much faster, and only involve a minor loss of efficiency in a likelihood context (Joe, 2005). Grazian and Liseo (2017) and Klein and Smith (2018) integrate out uncertainty for  $F_Y$  using a Bayesian non-parametric estimator, but find that this does not improve the accuracy of inference meaningfully. Here, we adopt a two-stage estimator, and use the adaptive kernel density estimator (KDE) of Shimazaki and Shinomoto (2010) to estimate  $F_Y$  in the first stage.

#### 3.1 Posterior evaluation

We follow George and McCulloch (1993) and subsequent authors, and evaluate the  $2^p$  atoms in the posterior of  $\boldsymbol{\gamma}$  using Markov chain Monte Carlo (MCMC). However, direct computation of the posterior mass function at Eq. (2) is slow because computing  $c_{\text{BVS}}$  requires numerical integration over  $g$ . We therefore pursue an alternative approach that also generates  $g$  as part of the MCMC scheme. To implement the sampler we express the likelihood conditional on  $g$ , which following Klein and Smith (2018) can be obtained in closed form by transforming to the (normalized) pseudo-response as follows. Let  $\mathbf{Z} = (Z_1, \dots, Z_n)' = \frac{1}{\sigma} S_\gamma \tilde{\mathbf{Z}}$ , where  $\tilde{\mathbf{Z}}$  is the pseudo-response at Eq. (5), then it follows from Section 2.2 that  $\mathbf{Z}|X, \boldsymbol{\gamma}, g \sim N(0, R(X, \boldsymbol{\gamma}, g))$ . Moreover,  $Y_i$  can be expressed in terms of  $Z_i$  as  $Y_i = F_Y^{-1}(\Phi_1(Z_i))$ , which is neither a function of  $X$  nor  $\boldsymbol{\gamma}$ . By a change of variables from  $\mathbf{Y}$  to  $\mathbf{Z}$ ,

$$p(\mathbf{y}|X, \boldsymbol{\gamma}, g) = p(\mathbf{z}|X, \boldsymbol{\gamma}, g) \prod_{i=1}^n \frac{p_Y(y_i)}{\phi_1(z_i)} = \phi(\mathbf{z}; \mathbf{0}, R) \prod_{i=1}^n \frac{p_Y(y_i)}{\phi_1(z_i)}, \quad (9)$$

where the Jacobian of the transformation is  $|\frac{d\mathbf{z}}{d\mathbf{y}}| = \prod_{i=1}^n \frac{p_Y(y_i)}{\phi_1(z_i)}$ .

The right-hand side of Eq. (9) is tractable, as long as the  $n \times n$  matrix  $R$  is not computed directly. To evaluate the posterior, we employ the following sampler.

#### MCMC Sampler

Step 1. Randomly partition  $\gamma$  into pairs of elements.

Step 2. For each pair  $(\gamma_i, \gamma_j)$ , generate from  $p(\gamma_i, \gamma_j | \{\gamma \setminus \gamma_i, \gamma_j\}, X, g, \mathbf{y})$ .

Step 3. Generate from  $p(g | X, \gamma, \mathbf{y})$  using Hamiltonian Monte Carlo.

In forming the partition in Step 1, if  $p$  is odd-valued one element is simply selected twice, so that pairs of elements  $(\gamma_i, \gamma_j)$  are always generated in Step 2. To implement Step 2, first note that from Eq. (9) the joint posterior of the indicators is

$$\begin{aligned} p(\gamma | X, g, \mathbf{y}) &\propto p(\mathbf{y} | X, \gamma, g) p(\gamma) \propto \phi(\mathbf{z}; \mathbf{0}, R(X, \gamma, g)) p(\gamma) \\ &\propto |R(X, \gamma, g)|^{-1/2} \exp \left\{ -\frac{1}{2} (\mathbf{z}' R(X, \gamma, g)^{-1} \mathbf{z}) \right\} \text{Beta}(p - q_\gamma + 1, q_\gamma + 1) \\ &\equiv A(\gamma_i, \gamma_j). \end{aligned}$$

Generating each pair  $(\gamma_i, \gamma_j)$  involves computing  $A$  for the four possible configurations  $(\gamma_i, \gamma_j) \in \mathcal{S} \equiv \{(0, 0), (0, 1), (1, 0), (1, 1)\}$ , and then setting

$$p((\gamma_i, \gamma_j) | \{\gamma \setminus (\gamma_i, \gamma_j)\}, X, g, \mathbf{y}) = \frac{1}{1+h}, \quad h = \sum_{(\tilde{\gamma}_i, \tilde{\gamma}_j) \in \{\mathcal{S} \setminus (\gamma_i, \gamma_j)\}} \frac{A(\tilde{\gamma}_i, \tilde{\gamma}_j)}{A(\gamma_i, \gamma_j)}, \quad (10)$$

where we are careful to compute all ratios on the logarithmic scale. To implement this efficiently requires fast computation of  $A$  for the four configurations in  $\mathcal{S}$ , which we do using a number of matrix identities, as outlined in Appendix B. In doing so, at no stage is the  $n \times n$  matrix  $R$  computed directly, which would be prohibitive.

Generating  $g$  at Step 3 uses a Hamiltonian Monte Carlo (HMC) step for  $\tilde{g} = \log(g)$ . This is where  $\tilde{g}$  is augmented by a momentum variable, and a draw is made from the extended target distribution that is proportional to the exponential of the Hamiltonian function. Dynamics specify how the Hamiltonian function evolves, and its volume-conserving property results in high acceptance rates of the proposed iterates. We use a variant of the leapfrog integrator of Neal (2011) to generate  $\tilde{g}$ , which employs the logarithm of the target density given by

$$l_{\tilde{g}} \equiv \log(p(\tilde{g} | X, \gamma, \mathbf{y})) \propto -\frac{1}{2} \sum_{i=1}^n \log(s_i^2) - \frac{q_\gamma}{2} \log(1 + \exp(\tilde{g})) + \tilde{g} - \frac{1}{2} \mathbf{z}' R^{-1} \mathbf{z} + \log(p(\exp(\tilde{g})))$$

where  $p(\exp(\tilde{g}))$  are the priors at and its gradient

$$\begin{aligned} \nabla_{\tilde{g}} l_{\tilde{g}} &= \exp(\tilde{g}) \left[ -\frac{1}{2} \sum_{i=1}^n \frac{\partial s_i^2}{\partial g} s_i^{-2} - \frac{q_\gamma}{2(1+g)} + \frac{1}{g} + \frac{1}{2(1+g)^2} \mathbf{z}' S^{-1} M_\gamma M_\gamma' S^{-1} \mathbf{z} \right. \\ &\quad \left. - \mathbf{z}' \frac{\partial S^{-1}}{\partial g} (I - \frac{g}{1+g} M_\gamma M_\gamma) S^{-1} \mathbf{z} \right] + \frac{\partial}{\partial \tilde{g}} \log(p(\exp(\tilde{g}))). \end{aligned}$$

where  $p(\exp(\tilde{g}))$  are the priors for  $g$ . The step size  $\epsilon$  and the number of leapfrog steps  $L$

in each sweep is set using the dual averaging approach of Hoffman and Gelman (2014) as follows. A trajectory length  $\iota = \epsilon L = 0.5$  is obtained by preliminary runs of the sampler using a small value of  $\epsilon$  (to ensure a small discretization error) and a large value of  $L$  (to move far). The dual averaging algorithm uses this trajectory length and adaptively changes  $\epsilon, L$  during  $M_{\text{adapt}} \leq M$  iterations of the complete sampler with  $M$  sweeps, in order to achieve a desired rate of acceptance  $\delta$ . In our examples we choose  $\delta = 0.75$ ; see Hoffman and Gelman (2014) for recommendations. A reasonable starting value for  $\epsilon$  is determined by Algorithm 4 of (Hoffman and Gelman, 2014).

## 3.2 Inference

The sampler above produces draws  $\{\boldsymbol{\gamma}^{[k]}, g^{[k]}; k = 1, \dots, K\}$  from the posterior distribution  $p(\boldsymbol{\gamma}, g|X, \mathbf{y})$  which can be used to compute posterior estimates as detailed below.

### 3.2.1 Variable selection

Variables can be selected using the marginal posteriors, which are estimated as

$$\Pr(\gamma_i = 1|X, \mathbf{y}) \approx \frac{1}{K} \sum_{k=1}^K \Pr(\gamma_i = 1|\{\boldsymbol{\gamma}^{[k]} \setminus (\gamma_i, \gamma_j)\}, X, g^{[k]}, \mathbf{y}).$$

To evaluate the term in this summation, at Step 2 of the sampler for the single pair  $(\gamma_i, \gamma_j)$  that contains  $\gamma_i$ , the following is computed

$$\Pr(\gamma_i = 1|\{\boldsymbol{\gamma} \setminus (\gamma_i, \gamma_j)\}, X, g, \mathbf{y}) = \frac{A(1, 0) + A(1, 1)}{A(0, 0) + A(1, 0) + A(0, 1) + A(1, 1)},$$

where the four values of the bivariate function  $A(\gamma_i, \gamma_j)$  are already computed at Step 2 of the sampler.

### 3.2.2 Predictive density

In general, direct evaluation of the predictive density of a new observation  $Y_{n+1}$  with covariates  $\mathbf{x}_{n+1}$  at Eq. (3) is computationally infeasible because evaluating  $c_{\text{BVS}}$  is also. However, the posterior predictive density at Eq. (4) can still be evaluated by conditioning on  $\boldsymbol{\beta}_\gamma$  and  $g$  as follows. Note that

$$p(y_{n+1}|X^+, \mathbf{y}) = \sum_{\boldsymbol{\gamma}} \int \int p(y_{n+1}|X^+, \boldsymbol{\beta}_\gamma, \boldsymbol{\gamma}, g, \mathbf{y}) p(\boldsymbol{\beta}_\gamma, \boldsymbol{\gamma}, g|X, \mathbf{y}) d(\boldsymbol{\beta}_\gamma, g). \quad (11)$$

The predictive density inside the integrals above can be obtained by considering a change of variables from  $Y_{n+1}$  to  $Z_{n+1} = \Phi_1^{-1}(F_Y(Y_{n+1}))$ , with Jacobian  $\frac{p_Y(y_{n+1})}{\phi_1(z_{n+1})}$ , as

$$p(y_{n+1}|X^+, \boldsymbol{\beta}_\gamma, \boldsymbol{\gamma}, g, \mathbf{y}) = p(z_{n+1}|X^+, \boldsymbol{\beta}_\gamma, g, \boldsymbol{\gamma}, \mathbf{z}) \frac{p_Y(y_{n+1})}{\phi_1(z_{n+1})}.$$

From Eq. (5),  $\tilde{Z}_{n+1}|\mathbf{x}_{\gamma,i}, \boldsymbol{\beta}_\gamma, \boldsymbol{\gamma}, g \sim N(\mathbf{x}'_{\gamma,n+1}\boldsymbol{\beta}_\gamma, \sigma^2)$  independently when conditioning on  $\boldsymbol{\beta}_\gamma$  (whereas the elements of  $\tilde{\mathbf{Z}}$  are dependent unconditional on  $\boldsymbol{\beta}_\gamma$ ). Then, because  $Z_{n+1} = \frac{s_{n+1}}{\sigma} \tilde{Z}_{n+1}$ ,

$$p(y_{n+1}|X^+, \boldsymbol{\beta}_\gamma, \boldsymbol{\gamma}, g, \mathbf{y}) = \frac{1}{s_{n+1}} \phi_1 \left( \frac{z_{n+1} - s_{n+1} \mathbf{x}'_{\gamma,n+1} \boldsymbol{\beta}_\gamma}{s_{n+1}} \right) \frac{p_Y(y_{n+1})}{\phi_1(z_{n+1})}, \quad (12)$$

where recall that  $\phi_1$  is a  $N(0, 1)$  density,  $s_{n+1} = (1 + g \mathbf{x}'_{\gamma,n+1} (X_\gamma' X_\gamma)^{-1} \mathbf{x}_{\gamma,n+1})^{-1}$ , and  $\mathbf{x}_{\gamma,n+1}$  are the elements of  $\mathbf{x}_{n+1}$  that correspond to  $\boldsymbol{\gamma}$ . Notice that  $\sigma^2$  cancels out in the above computation because it is unidentified in the copula, and plays no role in the predictions.

An expression for the posterior predictive density is obtained by plugging Eq. (12) into Eq. (11). The integrals and summation can be evaluated in the usual Bayesian fashion by averaging over Monte Carlo iterates from the posterior  $p(\boldsymbol{\beta}_\gamma, \boldsymbol{\gamma}, g|X, \mathbf{y})$ . However, this requires the additional generation of  $\boldsymbol{\beta}_\gamma$  at each sweep of the sampler. A faster approximation that avoids this—and which we have found to be almost as accurate empirically—is to plug in the posterior expectation of  $\boldsymbol{\beta}_\gamma$  given by,

$$\hat{\boldsymbol{\beta}}_\gamma \equiv \mathbb{E}(\boldsymbol{\beta}_\gamma|X, \boldsymbol{\gamma}, g, \mathbf{y}) = \frac{g}{1+g} (X_\gamma' X_\gamma)^{-1} X_\gamma' S_\gamma^{-1} \mathbf{z}.$$

Note that the main components required for the evaluation of  $\hat{\boldsymbol{\beta}}_\gamma$  have already been computed at each sweep of the sampler. Thus, a fast and accurate predictive density estimator can be constructed using the  $K$  Monte Carlo iterates from the sampler as

$$\hat{p}(y_{n+1}|X^+, \mathbf{y}) = \frac{\hat{p}_Y(y_{n+1})}{\phi_1(\Phi_1^{-1}(\hat{F}_Y(y_{n+1})))} \left\{ \frac{1}{K} \sum_{k=1}^K \frac{1}{s_{n+1}^{[k]}} \phi_1 \left( \frac{\Phi_1^{-1}(\hat{F}_Y(y_{n+1})) - s_{n+1}^{[k]} \mathbf{x}'_{\gamma^{[k]},n+1} \hat{\boldsymbol{\beta}}_{\gamma^{[k]}}}{s_{n+1}^{[k]}} \right) \right\}, \quad (13)$$

with  $s_{n+1}^{[k]} \equiv (1 + g^{[k]} \mathbf{x}'_{\gamma^{[k]},n+1} (X_{\gamma^{[k]}}' X_{\gamma^{[k]}})^{-1} \mathbf{x}_{\gamma^{[k]},n+1})^{-1}$ .

### 3.2.3 Regression function estimator

The regression function  $f(x_{n+1}) \equiv \mathbb{E}(Y_{n+1}|\mathbf{x}_{n+1})$  can be estimated using the posterior predictive mean

$$\hat{f}(\mathbf{x}_{n+1}) = \mathbb{E}(Y_{n+1}|X^+, \mathbf{y}) = \sum_{\boldsymbol{\gamma}} \int \int \mathbb{E}(Y_{n+1}|X^+, \boldsymbol{\beta}_\gamma, \boldsymbol{\gamma}, g, \mathbf{y}) p(\boldsymbol{\beta}_\gamma, \boldsymbol{\gamma}, g|X, \mathbf{y}) d(\boldsymbol{\beta}_\gamma, g). \quad (14)$$

The expectation in the integrand above can be computed by a change of variables from  $Y_{n+1}$  to  $Z_{n+1}$  and plugging in the expression at Eq. (12) to give

$$\mathbb{E}(Y_{n+1}|X^+, \boldsymbol{\beta}_\gamma, \boldsymbol{\gamma}, g, \mathbf{y}) = \int \frac{F_Y^{-1}(\Phi_1(z_{n+1}))}{s_{n+1}} \phi_1 \left( \frac{z_{n+1} - s_{n+1} \mathbf{x}'_{\gamma,n+1} \boldsymbol{\beta}_\gamma}{s_{n+1}} \right) dz_{n+1},$$

where the univariate integral with respect to  $z_{n+1}$  is computed numerically. Evaluation of Eq. (14) then proceeds by plugging in  $\hat{\beta}_\gamma$  and averaging over the Monte Carlo iterates in the exactly the same manner as in Section 3.2.2 above.

### 3.2.4 Bayes factor

Last, we derive the Bayes factor for a pair of hypothesized subsets  $\gamma$  and  $\tilde{\gamma}$ . For subset  $\gamma$ , let  $U_\gamma$  be a upper triangular Cholesky factor, such that  $U'_\gamma U_\gamma = X'_\gamma X_\gamma$  and  $M_\gamma = X_\gamma U_\gamma^{-1}$ . Then  $s_{i,\gamma} = (1 + g \sum_{j=1}^{q_\gamma} m_{\gamma,ij}^2)^{-1/2}$  for  $i = 1, \dots, n$ ,  $M_\gamma = \{m_{\gamma,ij}\}$  and  $R(X, \gamma, g)^{-1} = S_\gamma^{-1}(I - \frac{g}{1+g} M_\gamma M'_\gamma) S_\gamma^{-1}$ ; and similar for  $\tilde{\gamma}$

**Proposition 1.** *The Bayes factor comparing the model with varying dimension parameter  $\gamma$  with the one with  $\tilde{\gamma}$  is given by*

$$BF(\gamma|\tilde{\gamma}) = \int_0^\infty \prod_{i=1}^n \left[ (1 + g \sum_{j=1}^{q_\gamma} m_{\gamma,ij}^2)^{\frac{1}{2}} (1 + g \sum_{j=1}^{q_{\tilde{\gamma}}} m_{\tilde{\gamma},ij}^2)^{\frac{1}{2}} \right] (1 + g)^{-\frac{q_\gamma - q_{\tilde{\gamma}}}{2}} \\ \exp \left\{ -\frac{\mathbf{z}' S_\gamma^{-1} S_\gamma^{-1} \mathbf{z}}{2(1 + g)} (1 + g (1 - \tilde{R}_{\gamma,g}^2)) \right\} \exp \left\{ \frac{\mathbf{z}' S_{\tilde{\gamma}}^{-1} S_{\tilde{\gamma}}^{-1} \mathbf{z}}{2(1 + g)} (1 + g (1 - \tilde{R}_{\tilde{\gamma},g}^2)) \right\} p(g) dg,$$

where we call

$$\tilde{R}_{\gamma,g}^2 = 1 - \frac{\mathbf{z}' S_\gamma^{-1} (I - M_\gamma M'_\gamma) S_\gamma^{-1} \mathbf{z}}{\mathbf{z}' S_\gamma^{-1} S_\gamma^{-1} \mathbf{z}}$$

the implicit copula coefficient of determination, which (as opposed to the ordinary coefficient of determination) depends on  $g$  in the copula model.

Note that the expression for  $BF(\tilde{\gamma}|\gamma)$  involves a univariate integral which can be approximated numerically or using Laplace approximations, and that the term  $\prod_{i=1}^n \frac{p_Y(y_i)}{\phi_1(z_i)}$  cancels out in its derivation. A direct consequence of Proposition 1 is the following Corollary.

**Corollary 2.** *For the empty subset, with  $\gamma = \mathbf{0}$  and  $q_{\gamma_N} = 0$ , the Bayes factor for comparing model  $\gamma$  with the null model is*

$$BF(\gamma|\gamma_N) = \int_0^\infty \prod_{i=1}^n (1 + g \sum_{j=1}^{q_\gamma} m_{ij}^2)^{\frac{1}{2}} (1 + g)^{-\frac{q_\gamma}{2}} \exp \left\{ \frac{\mathbf{z}' \mathbf{z}}{2} \right\} \exp \left\{ -\frac{\mathbf{z}' S_\gamma^{-1} S_\gamma^{-1} \mathbf{z}}{2(1 + g)} (1 + g (1 - \tilde{R}_{\gamma,g}^2)) \right\} p(g) dg.$$

The proofs of Proposition 1 and Corollary 2 can be found in Appendix C.2.

## 4 Simulation Study

To illustrate the effectiveness of our approach we undertake a simulation study. We employ the copula model at Eq. (1) with non-parametric estimates of the margins  $\hat{F}_Y$ , and label

this ‘BVSC’ throughout the rest of the paper. We consider the four priors for  $g$  outlined in Section 2.2, giving four variants. We consider two benchmark methods using the same predictors. The first is that of Liang et al. (2008), which has Gaussian disturbances and the same hyperpriors for  $g$  (so that there are also four variants). To evaluate the posterior for this model we use a MCMC sampler similar to that described in Section 3.1, and label this as ‘BVS’. The second benchmark is the two-piece distribution approach of Rossell and Rubio (2018) as implemented in the R-package `mombf` and labelled ‘mombf’, where the product MOM (pMOM) non-local prior proposed by Johnson and Rossell (2012) is used for the non-zero coefficients. This framework allows for estimating posterior model probabilities with normal (N), asymmetric normal (AN), Laplace (L) and asymmetric Laplace (AL) errors, and we further label the benchmark by these distribution types. Posterior sampling is however only established for the normal error model.

## 4.1 Simulation Design

We generate  $n = 200$  observations of  $p = 20$  correlated covariates  $\mathbf{x} = (x_1, \dots, x_{20})' \sim N(\mathbf{0}, \Sigma)$ , where  $\Sigma = R'R$  and  $R$  is an upper triangular Cholesky factor with non-zero elements generated as  $N(0, 0.1)$ . The resulting  $(n \times 20)$  design matrix  $X$  is then mean-centered (so that  $\mathbf{1}'X = \mathbf{0}$ ), creating a correlated but numerically stable design. For  $j = 1, \dots, 20$ , we set  $\beta_j = 0$  with probability 0.75, otherwise we generate  $\beta_j$  from an equally-weighted mixture of the two normals  $N(1.025^2)$  and  $N(-1, 0.25^2)$ . Setting  $\boldsymbol{\beta} = (\beta_1, \dots, \beta_{20})'$ , observations of the dependent variable are generated from the following three distributions for  $i = 1, \dots, n$ :

$$\text{Case 1, Normal:} \quad Y_{1,i} = \mathbf{x}'_i \boldsymbol{\beta} + \varepsilon_{1,i}, \quad \varepsilon_{1,i} \sim N(0, r_1^2),$$

$$\text{Case 2, Log-normal:} \quad Y_{2,i} = \exp(\mathbf{x}'_i \boldsymbol{\beta} + 1.5\varepsilon_{2,i}), \quad \varepsilon_{2,i} \sim N(0, r_2^2),$$

$$\text{Case 3, Implicit Copula:} \quad Y_{3,i} = F_{\text{LN}}^{-1}(z_i; 3, 2), \quad z_i = \mathbf{x}'_i \boldsymbol{\beta} + \varepsilon_{3,i}, \quad \varepsilon_{3,i} \sim N(0, r_3^2),$$

where  $F_{\text{LN}}$  is the log-normal distribution function. The distribution in case 1 matches that of the Gaussian linear model (which is assumed in the BVS and `mombf`/N benchmarks), while that in case 3 matches that of the implicit copula model (ie. BVSC). The distribution in case 2 matches neither model. For each of the three cases we simulated  $K = 100$  datasets, which we refer to as replicates. To make the three cases comparable, we set  $r_1, r_2$  and  $r_3$  to values that give a signal-to-noise ratio (SNR) equal to 8. We define this ratio as  $\text{SNR}(r_j) = \text{range}(\mathbb{E}(Y_j|\mathbf{x}; r_j))/\text{Var}(Y_j|\mathbf{x}; r_j)^{1/2}$ , and refer to the Online Appendix for details on its computation. Solving the resulting nonlinear system for each  $r_j$  yields  $r_1 = 0.25$ ,



$r_2 = 1.5$  and  $r_3 = 0.60$ .

## 4.2 Results

To compare the approaches we consider two metrics. The first measures the accuracy of the predictive densities of the dependent variable, and second the correct selection of variables.

### 4.2.1 Prediction Accuracy

To measure the accuracy of the predictive density of the dependent variable we use the mean logarithmic score computed by ten-fold cross-validation. For a given replicate, we compute this by partitioning the data into ten equally sized sub-samples of sizes  $n_k$ , denoted here as  $\{(y_{i,k}, \mathbf{x}_{i,k}); i = 1, \dots, n_k\}$  for  $k = 1, \dots, 10$ . For each observation in sub-sample  $k$ , we compute the predictive density estimator at Eq. (13) using the remaining nine sub-samples as the training data, and denote these densities here as  $\hat{p}_k(y_{i,k}|\mathbf{x}_{i,k})$ . The ten-fold mean logarithmic score is then  $\text{MLS} = \frac{1}{10} \sum_{k=1}^{10} \frac{1}{n_k} \sum_{i=1}^{n_k} \log \hat{p}_k(y_{i,k}|\mathbf{x}_{i,k})$ .

Figure 1 gives boxplots of the MLS of the 100 replicates for the three cases in panels (a–c). In each panel, nine methods are considered: the four variants of both BVSC and BVS (ie. both methods implemented with the four different priors for  $g$ ) and  $\text{mombf}/N$ .<sup>2</sup> We make three observations. First, the results for the BVS are very robust with respect to choice of prior for  $g$ , whereas choosing  $g$  makes a bigger difference for BVSC. Second, while for the normal case 1 the BVS is slightly better than the BVSC, the BVSC outperforms both the BVS and  $\text{mombf}/N$  substantially in the two non-Gaussian cases. Last, in case 1 the  $\text{mombf}/N$  has the highest variance.

### 4.2.2 Selection Accuracy

The second measure is the precision-recall curve, which is a popular criterion for assessing classification in machine learning (Davis and Goadrich, 2006). Here, the classification problem is the selection from 20 covariates, based on the marginal posterior probabilities  $\Pr(\gamma_j = 1|\mathbf{y})$  produced by each method and for each case. Given a threshold probability value, let TP, FP and FN be true positive, false positive and false negative classification rates, respectively. Then the curve plots  $\text{Recall}=\text{TP}/(\text{TP}+\text{FN})$  on the horizontal axis, against  $\text{Precision}=\text{TP}/(\text{TP}+\text{FP})$  on the vertical axis, as the threshold probability value varies from 0 to

---

<sup>2</sup>The other distributional forms are not included here because posterior sampling is currently unavailable in the  $\text{mombf}$  package for these cases.

1. Simultaneously high values of Recall and Precision (ie. curves that look like a transposed letter ‘L’) indicate accurate classification.

Figure 2 plots the average precision-recall curves over the 100 replicates of the simulation study. The results for each of the three cases are given in the three rows of panels. For each case, a total of 12 precision-recall curves—one for each method and variant—are presented, and we make three observations. First, the asymmetric variants of the mombf perform very poorly whenever the normal assumption does not hold (in cases 2 and 3), despite allowing for asymmetry and skewness. Second, the BVSC is much more accurate in cases 2 and 3, where it also outperforms BVS for all variants of priors for  $g$ . This robustness to distributional form is a result of the flexibility obtained through the non-parametric calibration of the margins. Third, only for the known Gaussian data generating process (case 1) is the BVSC less accurate than the BVS and mombf alternatives; although the under-performance is minor when compared to the gains obtained in two non-Gaussian cases.

## 5 Print Advertising Example

To illustrate our approach we apply it to the print advertising data examined by Smith et al. (2000). The data were collected by a marketing research company, and concern the print advertisements (ads) that appeared in 13 issues of an Australian monthly magazine published between March 1992 and March 1993. The authors regress measures of attention to each ad, observed in a laboratory setting, against features of the ad. These include the ad’s position in the issue, design and message attributes, product category and magazine issue number, along with a large number of interaction effects. Here, we consider regressions of the dependent variable ‘noted score’ against the  $p = 252$  covariates proposed by the authors, which we label  $X_1, \dots, X_{252}$  here and list in the Online Appendix. Following Smith et al. (2000), we fit the model to the  $n = 943$  ads from the first 12 magazine issues, and then use it to predict the noted score of the 62 ads from the last issue. These authors also observe that many of the covariates are likely to be unimportant, and that the distribution of the dependent variable is also non-Gaussian. They undertake Bayesian variable selection with automatic data transformation identification using the approach outlined in Smith and Kohn (1996), and our analysis extends theirs.

A Shapiro-Wilk test rejects normality for the dependent variable, with a statistic of  $W = 0.996$  and  $p$ -value = 0.02. The KDE of  $F_Y$  for the first 12 magazine issues is given

in Figure 3, showing a mild deviation from normality. We estimate the BVSC parameters using all three priors for  $g$ . For comparison, we also estimate standard BVS with Gaussian disturbances and the same priors for  $g$  and  $\gamma$ . Table 1 reports mean in- and out-of-sample logarithmic scores computed for all models, and we make three observations. First, using both the in- and out-of-sample metrics, the BVSC model with a hyper- $g$  or hyper- $g/n$  prior is optimal. Second, these two copula models out-perform all BVS models substantially, suggesting that accounting for even a mild deviation from a Gaussian in the margin of  $Y$  can improve fit. Last, fixing  $g = 100$  works poorly, particularly with the BVSC model.

To illustrate the impact on variable selection, Table 2 reports the 30 variables with the highest posterior probabilities of selection  $\Pr(\gamma_i = 1|X, \mathbf{y})$  from the BVSC model with a hyper- $g$  prior. Also reported are the posterior probabilities of selection for the same variables from the other 7 models. The posterior mean  $\mathbb{E}(q_\gamma|X, \mathbf{y})$  and standard deviation  $\text{Var}(q_\gamma|X, \mathbf{y})^{1/2}$  of the number of terms are reported in the bottom rows. We make four observations. First, all models select the first three of these variables ( $X_{79}, X_{54}, X_{55}$ ). Second, the posterior probabilities for the remaining variables are very similar across the BVSC models, except when  $g = 100$ . Third, the variables selected by the copula models are very different from those selected using BVS with Gaussian disturbances. Thus, allowing for flexibility in the marginal distribution of the dependent variable can affect selection greatly. Last, the three most accurate copula models identify the largest sets of covariates, with around twice as many included than when using BVS with Gaussian disturbances.

## 6 Extension to Spatial BVS for fMRI

An important application of Bayesian variable selection is to construct activation maps in functional magnetic resonance imaging (fMRI) studies. This involves the extension of selection methods to spatial data located on a regular lattice of ‘voxels’ that partition the brain (Smith et al., 2003; Smith and Fahrmeir, 2007; Goldsmith et al., 2014; Lee et al., 2014). We show how to extend our method to this case, and demonstrate that the activation maps can be more accurate when taking into account the non-Gaussianity of the magnetic resonance (MR) signal using our copula-based approach to variable selection. This is consistent with recent work that suggests the MR signal is neither conditionally Gaussian nor homoscedastic (Eklund et al., 2017).

## 6.1 Marginally calibrated variable selection for fMRI

In fMRI studies, a MR signal  $\{Y_{i,t}; t = 1, \dots, T\}$  is observed at each voxel  $i \in \{1, \dots, N\}$ . This is matched with a series of observations  $\{x_{i,t}; t = 1, \dots, T\}$  on a transformed stimulus, which is a delayed and continuously modified version of an original stimulus, called the hemodynamic response function. The objective in such analyses is to identify at which voxels the MR signal is related to the transformed stimulus; see Gössl et al. (2001) and Bezener et al. (2018) for overviews.

Denote voxel activation by a vector of binary indicator variables  $\boldsymbol{\gamma} = (\gamma_1, \dots, \gamma_N)'$ , such that the  $i$ th voxel is activated by the stimulus if  $\gamma_i = 1$ , and inactivate if  $\gamma_i = 0$ . Spatial smoothing is essential to obtaining reliable activation maps, and we use the same Ising mass function as these authors as a prior, given by

$$p(\boldsymbol{\gamma}|\theta) \propto \exp \left( \sum_{i=1}^N \delta_i \gamma_i + \theta \sum_{i \sim j} \omega_{ij} \mathcal{I}(\gamma_i = \gamma_j) \right).$$

Here,  $\mathcal{I}(A) = 1$  if  $A$  is true and zero otherwise, and  $\omega_{ij}$  is a constant weight proportional to the inverse Euclidean distance between voxels  $i$  and  $j$ . The summation over  $i \sim j$  denotes a summation over all pairwise neighboring elements of  $\boldsymbol{\gamma}$  (which are given by the up to 8 immediate neighbors of each voxel in two dimensions, and 26 immediate neighbors in three dimensions), and the parameter  $0 \leq \theta \leq 0.45$  controls the level of spatial smoothing. The values  $\delta_1, \dots, \delta_N$  are constants fixed to represent the anatomy of the acquisition and to calibrate overall classification rates; see Smith and Fahrmeir (2007) and Lee et al. (2014) for further details on this prior.

To extend our copula model in Section 2.1 to this case, let  $\mathbf{Y}_i = (Y_{i,1}, \dots, Y_{i,T})'$ ,  $\mathbf{x}_i = (x_{i,1}, \dots, x_{i,T})'$ ,  $\mathbf{Y} = (\mathbf{Y}'_1, \dots, \mathbf{Y}'_N)'$  and  $\mathbf{x} = (\mathbf{x}'_1, \dots, \mathbf{x}'_N)'$ . Also, let  $\mathbf{w}_t = (w_{t,1}, \dots, w_{t,m})'$  be  $m$  basis functions (which we specify later) evaluated at time point  $t$  used to capture a localised baseline time trend, and  $W = [\mathbf{w}_1 | \dots | \mathbf{w}_T]'$ . Then, assuming  $Y_{i,t}$  is *marginally* independent of  $\mathbf{x}$ ,  $W$  and  $\boldsymbol{\gamma}$ , but voxel-specific with distribution function  $F_{Y_i}(y_{i,t})$  and density  $p_{Y_i}(y_{i,t})$ , we adopt the following copula decomposition for the *joint* density of  $\mathbf{Y}|\mathbf{x}, W, \boldsymbol{\gamma}$ :

$$p(\mathbf{y}|\mathbf{x}, W, \boldsymbol{\gamma}) = \prod_{i=1}^N \left( c_{\text{SBVS}}(\mathbf{u}_i|\mathbf{x}_i, W, \gamma_i) \prod_{t=1}^T p_{Y_i}(y_{i,t}) \right),$$

where  $\mathbf{u}_i = (u_{i,1}, \dots, u_{i,T})'$  and  $u_{i,t} = F_{Y_i}(y_{i,t})$ . For the  $T$ -dimensional copula density  $c_{\text{SBVS}}$  we employ an implicit copula derived from a pseudo-regression model, as outlined in Section 6.2 below.

Notice that conditional on  $\gamma$  the MR signals  $\mathbf{Y}_1, \dots, \mathbf{Y}_N$  are independent and identically distributed, yet spatial dependence is introduced in the posterior of  $\gamma$  through the hierarchical Ising prior, with

$$p(\gamma|\mathbf{x}, W, \gamma, \mathbf{y}) \propto \left( \prod_{i=1}^N c_{\text{SBVS}}(\mathbf{u}_i|\mathbf{x}_i, W, \gamma_i) \right) p(\gamma|\theta).$$

As in previous sections, variable selection (ie. the classification of voxels as active or inactive) using the posterior above is separated from the task of marginal calibration of the distributions  $F_{Y_1}, \dots, F_{Y_N}$  of the MR signal. We show later in our empirical work that this changes the activation maps and improves the quality of fit (as measured using mean logarithmic scores) substantially.

## 6.2 Spatial variable selection copula

We derive the copula density  $c_{\text{SBVS}}$  from a linear regression model in the same fashion as in Section 2.2. Because it is of the same form at every voxel, to simplify notation we drop the index  $i$  in this subsection only. In particular, for a pseudo-response  $\tilde{Z}_t$  we assume

$$\tilde{Z}_t = \mathbf{w}'_t \boldsymbol{\alpha} + x_t \beta(\gamma) + \varepsilon_t, \quad t = 1, \dots, T,$$

where  $\varepsilon_t \sim N(0, \sigma^2)$ ,  $\mathbf{w}'_t \boldsymbol{\alpha}$  is a time trend with eight low order Fourier terms as basis functions,  $x_t \beta(\gamma)$  is an activation effect with scalar amplitude  $\beta(\gamma)$ , and we label  $\beta$  as a function of  $\gamma$ , rather than use  $\gamma$  as a subscript as in earlier sections. It is usual to apply such a regression model directly to the MR signal at each voxel, but here we instead extract its implicit copula. Note that this regression is similar to that at Eq. (5), but with an additional time trend and where variable selection is performed on only the single coefficient  $\beta(\gamma)$  at each voxel.

Setting  $\tilde{\mathbf{Z}} = (\tilde{Z}_1, \dots, \tilde{Z}_T)'$ , the regression can be written as the linear model

$$\tilde{\mathbf{Z}} = W \boldsymbol{\alpha} + \mathbf{x} \beta(\gamma) + \boldsymbol{\varepsilon}, \tag{15}$$

with  $\boldsymbol{\varepsilon} = (\varepsilon_1, \dots, \varepsilon_T)'$ . Proper priors have to be employed for  $\boldsymbol{\alpha}$  and  $\beta(\gamma = 1)$  to obtain a proper implicit copula. We use the same spike-and-slab prior for the amplitude as previously, which can be written for this scalar as  $\beta(\gamma = 0) = 0$ , and  $\beta(\gamma = 1)|g, \sigma^2 \sim N(0, g\sigma^2(\mathbf{x}'\mathbf{x})^{-1})$ , where  $g$  is assumed common across all voxels. We use a  $N(0, \sigma^2 dI)$  prior for  $\boldsymbol{\alpha}$ , with  $d$  chosen to make the prior relatively uninformative, along with the same four priors for  $g$  used previously.

The same process is used to construct  $c_{\text{SBVS}}$  as in Section 2.2, but tailored to Eq. (15).

First, the joint distribution  $\tilde{\mathbf{Z}}|\mathbf{x}, W, \gamma, g, \sigma^2 \sim N(\mathbf{0}, \Omega)$ , with

$$\Omega = \sigma^2 \left( I + dWW' + \mathcal{I}(\gamma = 1) \frac{g\mathbf{x}\mathbf{x}'}{\mathbf{x}'\mathbf{x}} \right),$$

where  $\beta(\gamma)$  and  $\boldsymbol{\alpha}$  have been integrated out analytically as Gaussians, and the Woodbury formula applied; see the Online Appendix for details. Second, the pseudo-response is standardized by the marginal variances of this distribution to give  $\mathbf{Z} = \sigma^{-1}S\tilde{\mathbf{Z}}$ , with  $S = \text{diag}(s_1(\gamma), \dots, s_T(\gamma))$  and

$$s_t(\gamma) = \left( 1 + d\mathbf{w}'_t\mathbf{w}_t + \mathcal{I}(\gamma = 1) \frac{gx_t^2}{\mathbf{x}'\mathbf{x}} \right)^{-\frac{1}{2}}.$$

Thus,  $\mathbf{Z}|\mathbf{x}, W, \gamma, g, \sigma^2 \sim N(\mathbf{0}, R(\mathbf{x}, W, \gamma, g))$ , where

$$R(\mathbf{x}, W, \gamma, g) = S \left( I + dWW' + \mathcal{I}(\gamma = 1) \frac{g\mathbf{x}\mathbf{x}'}{\mathbf{x}'\mathbf{x}} \right) S, \quad (16)$$

is a correlation matrix, and the implicit copula of both  $\tilde{\mathbf{Z}}$  and  $\mathbf{Z}$  (conditional on  $\mathbf{x}, W, \gamma, g, \sigma^2$ ) is a Gaussian copula with parameter matrix  $R$  at Eq. (16). Finally, we obtain  $c_{\text{SBVS}}$  by mixing over the prior for  $g$ , which we formalize in the following definition.

**Definition 2.** Let  $c_{G_a}$  be the Gaussian copula density with correlation matrix  $R$  at Eq. (16).

If  $p(g)$  is a proper prior density for  $g > 0$ , then we call

$$c_{\text{SBVS}}(\mathbf{u}|\mathbf{x}, W, \gamma) = \int c_{G_a}(\mathbf{u}; R(\mathbf{x}, W, \gamma, g))p(g)dg.$$

the density function of a spatial variable selection copula.

It follows from Corollary 1 that the function  $c_{\text{SBVS}}$  is a well-defined copula density. As before,  $R$  is not a function of  $\sigma^2$ , so that  $\sigma^2$  is unidentified in the copula and does not feature in its definition.

### 6.3 Estimation and inference

Parameter estimation and posterior inference is obtained using an adaptation of the sampler in Section 3.1. It is a single-site sampler in the elements of  $\boldsymbol{\gamma} = (\gamma_1, \dots, \gamma_N)'$ , which is more computationally efficient than multi-site samplers (eg. Nott and Green (2004)) because key quantities can be pre-computed just once. As Smith et al. (2003) and Goldsmith et al. (2014) observe, this is important when undertaking variable selection in fMRI studies due to the large number of voxels  $N$ .

#### MCMC Sampler for Spatial Variable Selection Copulas

Step 1. Generate from  $p(\gamma_i|\{\boldsymbol{\gamma}\setminus\gamma_i\}, \mathbf{x}, W, g, \theta, \mathbf{y})$  for  $i \in \{1, \dots, N\}$  in random order.

Step 2. Generate from  $p(g|\mathbf{x}, W, \boldsymbol{\gamma}, \mathbf{y})$  using a Metropolis-Hastings step.

Step 3. Generate from  $p(\theta|\boldsymbol{\gamma}, \mathbf{y})$  using a Metropolis-Hastings step.

To implement Step 1 first note that if  $L_i(\gamma_i) \propto p(\mathbf{y}_i|\mathbf{x}_i, W, \gamma_i, g)$ , then

$$p(\boldsymbol{\gamma}|\mathbf{x}, W, g, \theta, \mathbf{y}) \propto \left( \prod_{i=1}^N L_i(\gamma_i) \right) p(\boldsymbol{\gamma}|\theta) \equiv A(\boldsymbol{\gamma})$$

and  $p(\gamma_i = 1|\{\boldsymbol{\gamma}\setminus\gamma_i\}, \mathbf{x}, W, g, \theta, \mathbf{y}) = 1/(1 + h_i)$ , where

$$\log h_i = \log A(\gamma_i = 0) - \log A(\gamma_i = 1) = -\delta_i + l_i + \theta \sum_{j \sim i} \omega_{ij}(1 - 2\gamma_j),$$

and  $l_i = \log \left( \frac{L_i(\gamma_i=0)}{L_i(\gamma_i=1)} \right)$ . Appendix D outlines how to compute  $l_i$  efficiently. In doing so,  $L_i(\gamma_i = 0)$  has to be computed only once for each voxel, and at no stage do any of the  $N$  correlation matrices  $\{R(\mathbf{x}_i, W, \gamma_i, g); i = 1, \dots, N\}$  (each of which is  $T \times T$ ) need to be computed or factored directly.

Generating  $g$  at Step 2 uses a Metropolis-Hastings step for  $\tilde{g} = \log(g)$ , rather than a HMC step as in Section 3.1. This is because the former yields improved mixing, with acceptance rates between 80–95% in our empirical work. A proposal  $\tilde{g}^{(\text{new})}$  is generated from  $N(\tilde{g}^*, 1/h^*)$ , where  $\tilde{g}^*$  is the minimum of

$$\begin{aligned} -p(\tilde{g}|\mathbf{x}, W, \boldsymbol{\gamma}, \mathbf{y}) &= -\sum_{i=1}^N \log L_i(\gamma_i) + \tilde{g} + \log p(\exp(\tilde{g})) \\ &= \sum_{i=1}^N (\mathcal{I}(\gamma_i = 1) \log L_i(\gamma_i = 1) + \mathcal{I}(\gamma_i = 0) \log L_i(\gamma_i = 0)) + \tilde{g} + \log p(\exp(\tilde{g})), \end{aligned}$$

and  $h^*$  is its second derivative evaluated at this minimum. Optimization is numerical, as is the computation of the second derivative. To generate  $\theta$  at Step 3 we use the same random-walk Metropolis-Hastings step outlined in Smith and Fahrmeir (2007). This approximates the normalizing constant of the Ising density using fast thermodynamic integration as in (Green and Richardson, 2002).

Monte Carlo mixture estimates of the marginal posteriors  $\Pr(\gamma_i = 1|\mathbf{x}, W, \mathbf{y})$  can be evaluated readily using the conditional posteriors in Step 1. These form the Bayesian estimates of the activation maps. An accompanying output is the map of posterior means of the amplitudes  $\beta_1, \dots, \beta_N$ . If  $(\boldsymbol{\gamma}^{[k]}, g^{[k]}, \theta^{[k]})$  is draw  $k$  from the joint posterior of  $(\boldsymbol{\gamma}, g, \theta)$ , then a Monte Carlo mixture estimate is

$$\mathbb{E}(\beta_i|\mathbf{x}, W, \mathbf{y}) \approx \frac{1}{K} \sum_{k=1}^K \mathbb{E}(\beta_i(\gamma_i^{[k]})|\mathbf{x}_i, W, g^{[k]}, \mathbf{y}_i),$$

which can be computed readily because at each sweep of the sampler because  $\mathbb{E}(\beta_i(\gamma_i =$

$0)|\mathbf{x}_i, W, g) = 0$  and

$$\mathbb{E}(\beta_i(\gamma_i = 1)|\mathbf{x}_i, W, g) = (\mathbf{x}'_i \mathbf{x}_i / g + \mathbf{x}'_i (I + dWW')^{-1} \mathbf{x}_i)^{-1} \mathbf{x}'_i (I + dWW')^{-1} S_i(\gamma_i = 1)^{-1} \mathbf{z}_i;$$

see the Online Appendix for detailed derivation.

## 6.4 Empirical results

To illustrate, we construct activation maps for slice 10 of individual B in Smith et al. (2003). This is an acquisition of a MR signal at 63 time points over  $72 \times 86$  voxels from a simple visual experiment. Activation is therefore largely in the visual cortex. Figure 4 plots the first four sample moments of the MR time series at each voxel, indicating a considerable deviation from normality. In particular, the higher order moments in panels (c) and (d) exhibit strong spatial dependence – something that is ignored in the Gaussian spatial Bayesian variable selection model (labelled ‘SBVS’ here) of Smith et al. (2003) and Smith and Fahrmeir (2007). Our spatial Bayesian variable selection *copula* model (labelled ‘SBVSC’ here) captures this through accurate calibration of the margins  $F_{Y_1}, \dots, F_{Y_N}$  using non-parametric estimators.

We estimate the SBVSC parameters for all four priors for  $g$ . For comparison, we also estimate the SBVS model of Smith and Fahrmeir (2007) using the same priors for  $g, \theta, \gamma$  as in the copula model. To compare the two sets of results, Table 3 reports the mean (in-sample) logarithmic scores for both the SBVS and SBVSC models, and for each prior of  $g$ . To compute these we evaluate the mean in-sample logarithmic scores at each voxel  $i$  as  $1/T \sum_{t=1}^T \log(\hat{p}(y_{i,t}|\mathbf{x}))$ , and then average the results across active, inactive and all voxels. We make two observations. First, in all cases the SBVSC scores are consistently higher across voxels than those for SBVS. The relative improvement is 9.5% for voxels classified as active by SBVSC, and 2% across all voxels. Second, these results are robust with respect to prior choice for  $g$ . In fact, the choice of prior for  $g$  has little impact on the posterior here. This is because at each voxel the  $g$ -prior is placed only on a single scalar  $\beta_i$ .

Based on these observations, Figure 5 compares activation and amplitude maps for three cases: panels (a,d) SBVSC with hyper- $g/n$  prior; (b,e) SBVS with hyper- $g/n$  prior; and (c,f) SBVS with  $g = 100$ . The latter case is included because it is the benchmark model suggested by Smith and Fahrmeir (2007). The activation maps in the first row are obtained by defining a voxel as active if and only if  $\Pr(\gamma_i = 1|\mathbf{x}, W, \mathbf{y}) \geq 0.8722$ . The justification for this threshold value is that  $-2 \log((1 - \Pr(\gamma_i = 1|\mathbf{x}, W, \mathbf{y}))/\Pr(\gamma_i = 1|\mathbf{x}, W, \mathbf{y}))$  is approximately  $\chi^2(1)$  distributed and the threshold corresponds to a p-value of 0.05 (Raftery, 1996). The



maps for the two SBVS models are close to identical, while they differ from those for the SBVSC model, with the latter allowing for sharper edges in the amplitude maps. To further highlight this difference, Figure 6 plots the difference in the activation probabilities between the copula and Gaussian models. These differ between -0.6 and 0.6, so that allowing for more accurate marginal calibration of the MR signal not only increases the logarithmic scores, but affects activation maps, which are the primary output of fMRI processing.

Both samplers were implemented efficiently in MATLAB. The time to undertake 1000 sweeps was approximately 10 mins (SBVS) and 11 mins (SBVSC) when  $g$  is generated, and 2 mins (SBVS) and 2.3 mins (SBVSC) when  $g$  is fixed. Thus, marginally-calibrated spatial BVS is only slightly slower than standard spatial BVS, and can be made even faster using a lower level language, as reported by Smith and Fahrmeir (2007). Typically, only a few thousand sweeps are needed to obtain highly accurate maps.

## 7 Discussion

This paper proposes a new tractable and general approach to undertake variable selection for non-Gaussian data. It uses a copula decomposition that ensures the marginal distribution of the dependent variable is always calibrated accurately; something that is hard to achieve otherwise. The key ingredient of the approach is a new family of implicit copula functions that are constructed from a hierarchical model for a Gaussian pseudo-response with spike-and-slab priors. These mix over the priors proposed by Liang et al. (2008) for the scaling factor of the  $g$  prior. This produces a family of copulas with dependence structures that are different than that of the Gaussian copula. Our empirical work demonstrates that mixing over such priors for  $g$  is important to allow for more accurate covariate selection and predictive densities of the dependent variable. We apply our approach to real data examples with  $p = 252$  correlated covariates and 6192 spatially correlated indicators, although it is applicable to much higher dimensions. This is because exact estimation by stochastic search over  $\gamma$  is fast when exploiting the matrix identities in Appendix B. The extension of the method to spatial Bayesian variable selection for fMRI—an important contemporary application (Bezener et al., 2018)—highlights its tractability.

While the use of copulas to capture dependence between multiple observations on one or more variables is rare, there are some recent examples. In regression these include implicit copulas constructed from Gaussian processes (Wilson and Ghahramani, 2010; Wauthier and

Jordan, 2010) or regularized basis functions (Klein and Smith, 2018). In time series analysis, both Gaussian and vine copulas have been used to capture serial dependence in univariate and multivariate data; for examples, see Smith (2015) and Brechmann and Czado (2015). These studies all exploit a copula decomposition to allow for non-Gaussian margins. However, ours is the first study to employ our proposed copula formulation to undertake variable selection.

We finish with some suggestions on future work. Copula models are extremely flexible and can also be used for capturing dependence in discrete or mixed data (Nelsen, 2006, p.43). Our proposed copula family can also be used in such a model, thereby extending Bayesian variable selection methods to discrete-valued dependent variables. Estimation can be undertaken using MCMC data augmentation as discussed by (Pitt et al., 2006), or variational methods. Another potential extension is to multivariate regression (ie. where there are multiple dependent variables), where Bayesian variable selection using spike-and-slab priors has been employed successfully for Gaussian data (Smith and Kohn, 2000; Brown et al., 2002). Here, the specification of an implicit copula analogous to that in Definition 1 would be required.

## Appendix A Margin of a Gaussian Linear Model

This appendix sketches the proof that in the Gaussian linear model  $\mathbf{Y}|X, \boldsymbol{\beta}, \sigma^2 \sim N(X\boldsymbol{\beta}, \sigma^2 I_n)$  with standard proper g-prior  $\boldsymbol{\beta}|\sigma^2 \sim N(\mathbf{0}, g\sigma^2(X'X)^{-1})$  and inverse gamma prior  $\sigma^2 \sim \text{IG}(a, b)$ , the marginal distribution  $Y_i|X$  (i.e. unconditional on  $\boldsymbol{\beta}$  and  $\sigma^2$ ) is asymptotically independent of  $X$ .

First, integrating out  $\boldsymbol{\beta}$  (as a Gaussian) gives the well-known result that  $\mathbf{Y}|X, \sigma^2 \sim N(\mathbf{0}, \sigma^2 \Sigma_n)$ , where

$$\Sigma_n = \left( I_{n \times n} - \frac{g}{1+g} X(X'X)^{-1}X' \right)^{-1} = I_{n \times n} + gX(X'X)^{-1}X',$$

with the last equality following from the Woodbury formula. The density of  $\mathbf{Y}|X$  is therefore

$$\begin{aligned} p(\mathbf{y}|X) &= \int p(\mathbf{y}|X, \sigma^2)p(\sigma^2)d\sigma^2 \\ &\propto \int (\sigma^2)^{-n/2-a-1} \exp\left(-b - \frac{1}{2\sigma^2}\mathbf{y}'\Sigma_n^{-1}\mathbf{y}\right) d\sigma^2 \end{aligned}$$

The integrand is the kernel of an  $\text{IG}(\tilde{a}, \tilde{b})$  distribution with parameters  $\tilde{a} = a + n/2$  and  $\tilde{b} = b + \frac{1}{2}\mathbf{y}'\Sigma_n^{-1}\mathbf{y}$ . The (inverse of the) normalizing constant of this distribution is

$$\Gamma(\tilde{a})\tilde{b}^{-\tilde{a}} = \Gamma(n/2 + a) \left( 1 + \frac{1}{2a}\mathbf{y}' \left( \frac{b}{a}\Sigma_n \right)^{-1} \mathbf{y} \right)^{-(n+2a)/2}.$$

Thus,  $p(\mathbf{y}|X)$  is the density of a multivariate t distribution with  $2a$  degrees of freedoms, zero mean and dispersion matrix  $\frac{b}{a}(I_n + X(X'X)^{-1}X')$ . Assuming that  $X \in \mathbb{R}^{n \times p}$  with  $p$  fixed,  $X$  has full column rank  $p$  and does not contain an intercept, then  $X(X'X)^{-1}X'$  approaches zero, see for instance (Christensen, 2011, Chapter 4.1). Hence,  $\frac{b}{a}(I_n + X(X'X)^{-1}X')$  will be close to  $\frac{b}{a}I_n$  for large  $n$ , so that the margin

$$Y_i|X \stackrel{a}{\sim} t(2a, 0, b/a),$$

which is not a function of any element of  $X$ .

## Appendix B Computational Details for the BVSC

This appendix outlines how to compute the posterior mass function at Eq. (10) efficiently. It shows how to evaluate  $A(\gamma_i, \gamma_j)$  quickly for the four configurations of  $(\gamma_i, \gamma_j) \in \mathcal{S}$ , using the following matrix computations. For  $k \in \{0, 1\}$ , let  $\boldsymbol{\gamma}^{(k)} = (\gamma_1, \dots, \gamma_{l-1}, k, \gamma_{l+1}, \dots, \gamma_p)$ ,  $U_k$  be an upper triangular Cholesky factor such that  $U_k'U_k = X'_{\gamma^{(k)}}X_{\gamma^{(k)}}$ , and  $M_k = X_{\gamma^{(k)}}U_k^{-1}$  be an  $n \times q_{\gamma^{(k)}}$  matrix. If  $\gamma_l = 0$ , then  $U_1$  can be readily computed from  $U_0$  using Cholesky updating in  $O(q_{\gamma^{(1)}}^2)$  operations, and  $M_1$  evaluated by solving the system of  $M_1U_1 = X_{\gamma^{(1)}}$ .

Similarly, if  $\gamma_l = 1$ , then  $U_0$  can be readily computed from  $U_1$  using Cholesky down-dating in  $O(q_{\gamma(0)}^2)$  operations, and  $M_0$  evaluated by solving the system of  $M_0 U_0 = X_{\gamma(0)}$ . These relationships allow rapid computation of the Cholesky factor  $U$  (such that  $U'U = X_\gamma' X_\gamma$ ) and  $M = X_\gamma U^{-1}$  for each of the four configurations of  $\gamma$ , because they only differ by up to two elements.

Given these matrices, for each configuration we compute:

- (i)  $s_i = (1 + g \sum_{j=1}^{q_\gamma} m_{ij}^2)^{-1/2}$  for  $i = 1, \dots, n$ , and set  $\tilde{\mathbf{z}} = (\tilde{z}_1, \dots, \tilde{z}_n)'$ , where  $\tilde{z}_i = z_i/s_i$  and  $M = \{m_{ij}\}$ ;
- (ii)  $\mathbf{z}'R(\mathbf{x}, \gamma)^{-1}\mathbf{z} = \tilde{\mathbf{z}}'(I - \frac{c}{1+c}MM')\tilde{\mathbf{z}}$  by solving  $\zeta = M'\tilde{\mathbf{z}}$ ; and,
- (iii)  $|R(X, \gamma, g)| = (\prod_{i=1}^n s_i^2)|I + gMM'| = (\prod_{i=1}^n s_i^2)|I + gM'M| = (\prod_{i=1}^n s_i^2)(1 + g)^{q_\gamma}$ ,<sup>3</sup>

The terms above are the main components required to compute  $A(\gamma_i, \gamma_j)$  for each configuration. Note that at no stage is either  $R$  or  $MM' = X_\gamma(X_\gamma'X_\gamma)^{-1}X_\gamma'$  computed directly, which would be prohibitive because they are both  $n \times n$  matrices.

## Appendix C Derivations and Proofs

### C.1 Derivation of dependence metrics in Section 2.3

To derive the lower quantile dependence metric at part (i),

$$\lambda_{ij}^L(q|X, \gamma) = \frac{C_{\text{BVS}}^{ij}(q, q)}{q} = \int \frac{C_{\text{Ga}}^{ij}(q, q) p(g)}{q} dg = \int \lambda_{\text{Ga}}^L(q|X, \gamma, g) p(g) dg.$$

The derivation of the upper quantile dependence is similar.

To derive the metrics at part (ii), first note that for any bivariate copula function  $C$ , if  $M(u, v) = \max(u, v)$  is the upper Fréchet-Hoeffding bound, then  $|C(q, q)/q| \leq M(q, q)/q = 1$ . Denote the  $(i, j)$ th element of  $R$  at Eqn. (7) as  $r_{ij}$ , and the sub-copulas of  $C_{\text{Ga}}$  and  $C_{\text{BVS}}$  in these elements as  $C_{\text{Ga}}^{ij}$  and  $C_{\text{BVS}}^{ij}$ . Then, by Proposition 1 and Lebesgue's dominated convergence theorem,

$$\lambda_{ij}^L = \lim_{q \downarrow 0} \frac{C_{\text{BVS}}^{ij}(q, q)}{q} = \int \lim_{q \downarrow 0} \frac{C_{\text{Ga}}^{ij}(q, q)}{q} p(g) dg = 0$$

because  $C_{\text{Ga}}^{ij}$  is a Gaussian copula with zero tail dependence, so that  $\lim_{q \downarrow 0} \frac{C_{\text{Ga}}^{ij}(q, q)}{q} = 0$ . The derivation of  $\lambda^U$  is similar.

The derivation of  $\rho_{ij}^S$  in part (iii) follows from the definition of Spearman's correlation,

---

<sup>3</sup>This follows from Sylvester's determinant identity.

and its expression for a Gaussian copula, as follows:

$$\begin{aligned}
\rho_{ij}^S(X, \gamma) &= 12 \int C_{\text{BVS}}^{ij}(u, v) d(u, v) - 3 = 12 \int \int C_{\text{Ga}}^{ij}(u, v) p(g) d(u, v) dg - 3 \\
&= \int \left( 12 \int C_{\text{Ga}}^{ij}(u, v) d(u, v) - 3 + 3 \right) p(g) dg - 3 \\
&= \frac{6}{\pi} \int \arcsin(r_{ij}/2) p(g) dg.
\end{aligned}$$

The derivation of  $\tau_{ij}^K$  in part (iv) is similar.

## C.2 Proofs of Proposition 1 and Corollary 2

For model  $\gamma$  the marginal distribution

$$\begin{aligned}
p(\mathbf{y}|X, \gamma, g) &= (2\pi)^{-\frac{n}{2}} \prod_{i=1}^n (1 + g \sum_{j=1}^{q_\gamma} m_{\gamma, ij}^2)^{\frac{1}{2}} (1 + g)^{-\frac{q_\gamma}{2}} \\
&\quad \exp \left\{ -\frac{\mathbf{z}' S_\gamma^{-1} S_\gamma^{-1} \mathbf{z}}{2(1 + g)} (1 + g(1 - \tilde{R}_{\gamma, g}^2)) \right\} \prod_{i=1}^n \frac{p_Y(y_i)}{\phi_1(z_i)}.
\end{aligned}$$

If  $\gamma \equiv \gamma_N = \emptyset$ , the marginal distribution  $p(\mathbf{y}|X, \gamma_N)$  simplifies to

$$p(\mathbf{y}|X, \gamma_N) = (2\pi)^{-\frac{n}{2}} \exp \left\{ -\frac{\mathbf{z}' \mathbf{z}}{2} \right\} \prod_{i=1}^n \frac{p_Y(y_i)}{\phi_1(z_i)}.$$

## Appendix D Fast Implementation of the SBVSC Sampler

We outline here how to implement Step 1 of the sampler in Section 6 quickly. First, denote  $R_i(\gamma_i) \equiv R(\mathbf{x}_i, W, \gamma_i, g)$  where the matrix  $R$  is defined in Eq. (16). Then the terms  $W'W$ ,  $d\mathbf{w}'_t \mathbf{w}_t$  and  $\mathbf{x}'_{it} (\mathbf{x}'_i \mathbf{x}_i)^{-1} \mathbf{x}_{it}$  for  $t = 1, \dots, T$ ,  $i = 1, \dots, N$  can all be pre-computed. Furthermore, for each voxel  $i = 1, \dots, N$ , the term

$$L_i(\gamma_i = 0) \propto |R_i(\gamma_i = 0)|^{-\frac{1}{2}} \exp \left( -\frac{1}{2} \mathbf{z}'_i R_i(\gamma_i = 0)^{-1} \mathbf{z}_i \right)$$

can also be pre-computed just once and quickly using the following expressions for the components of the calculation:

- i)  $S_i(\gamma_i = 0) = \text{diag}(s_{i,1}(\gamma_i = 0), \dots, s_{i,T}(\gamma_i = 0))$ , where  $s_{i,t}(\gamma_i = 0) = (1 + d\mathbf{w}'_t \mathbf{w}_t)^{-\frac{1}{2}}$ ;
- ii)  $R_i(\gamma_i = 0) = S_i(\gamma_i = 0)[I + dWW']S_i(\gamma_i = 0)$ ;
- iii)  $|R_i(\gamma_i = 0)| = \prod_{i=1}^T s_{i,t}(\gamma_i = 0)^2 |I_T + dWW'| = \prod_{i=1}^T s_{i,t}(\gamma_i = 0)^2 |I_m + dW'W|$ , which follows from Sylvester's determinant identity and that  $W$  is  $T \times m$  with  $m \ll T$ ; and,

iv) set  $\tilde{z}_{i,t} = \frac{z_{i,t}}{s_{i,t}(\gamma_i=0)}$ ,  $U'_0 U_0 = \left(\frac{1}{d}I + W'W\right)$  and  $M_0 = WU_0^{-1}$ . Then

$$\begin{aligned} \mathbf{z}'_i R_i(\gamma_i = 0)^{-1} \mathbf{z}_i &= \tilde{\mathbf{z}}'_i \left[ I - W \left( \frac{1}{d}I + W'W \right)^{-1} W' \right] \tilde{\mathbf{z}}_i \\ &= \tilde{\mathbf{z}}'_i \tilde{\mathbf{z}}_i - \tilde{\mathbf{z}}'_i \left[ W \left( \frac{1}{d}I + W'W \right)^{-1} W' \right] \tilde{\mathbf{z}}_i \\ &= \tilde{\mathbf{z}}'_i \tilde{\mathbf{z}}_i - \boldsymbol{\zeta}'_0 \boldsymbol{\zeta}_0, \end{aligned}$$

where one can solve  $\boldsymbol{\zeta}_0 = M'_0 \tilde{\mathbf{z}}_i$  quickly.

For each voxel  $i = 1, \dots, N$ , when  $\gamma_i = 1$ ,

$$L_i(\gamma_i = 1) \propto |R_i(\gamma_i = 1)|^{-\frac{1}{2}} \exp \left( -\frac{1}{2} \mathbf{z}'_i R_i(\gamma_i = 1)^{-1} \mathbf{z}_i \right)$$

needs to be updated at each sweep of the sampler because  $R_i(\gamma_i = 1)$  is a function of  $g$ . However, fast evaluation can be achieved by employing the following expressions for the component calculations:

- i)  $S_i(\gamma_i = 1) = \text{diag}(s_{i,1}(\gamma_i = 1), \dots, s_{i,T}(\gamma_i = 1))$ , with  $s_{i,t}(\gamma_i = 1) = \left( s_{i,t}(\gamma_i = 0)^{-2} + \frac{g x_{i,t}^2}{\mathbf{x}'_i \mathbf{x}_i} \right)^{-\frac{1}{2}}$ ;
- ii)  $R_i(\gamma_i = 1) = S_i(\gamma_i = 1) \left[ I + dW'W + g \frac{\mathbf{x}_i \mathbf{x}'_i}{\mathbf{x}'_i \mathbf{x}_i} \right] S_i(\gamma_i = 1)$ ;
- iii)  $|R_i(\gamma_i = 1)| = \prod_{i=1}^T s_{it,1}^2 |I + dWW' + g \frac{\mathbf{x}_i \mathbf{x}'_i}{\mathbf{x}'_i \mathbf{x}_i}|$ , where because  $W$  is a  $T \times m$  matrix, with  $T \gg m$ , the determinant can be computed efficiently as

$$\begin{aligned} \left| I_T + dWW' + g \frac{\mathbf{x}_i \mathbf{x}'_i}{\mathbf{x}'_i \mathbf{x}_i} \right| &= \left| I_T + \left[ \sqrt{d}W \sqrt{\frac{g}{\mathbf{x}'_i \mathbf{x}_i}} \mathbf{x}_i \right] \left[ \sqrt{d}W \sqrt{\frac{g}{\mathbf{x}'_i \mathbf{x}_i}} \mathbf{x}_i \right]' \right| \\ &= \left| I_{m+1} + \left[ \sqrt{d}W \sqrt{\frac{c}{\mathbf{x}'_i \mathbf{x}_i}} \mathbf{x}_i \right]' \left[ \sqrt{d}W \sqrt{\frac{g}{\mathbf{x}'_i \mathbf{x}_i}} \mathbf{x}_i \right] \right|; \end{aligned}$$

and

- iv) set  $\tilde{z}_{i,t} = \frac{z_{i,t}}{s_{i,t}(\gamma_i=1)}$  and  $U_1$  the Cholesky decomposition of  $\Sigma_i = I + dWW' + g \frac{\mathbf{x}_i \mathbf{x}'_i}{\mathbf{x}'_i \mathbf{x}_i}$  from above, such that  $U'_1 U_1 = \Sigma$  and  $M_1 = U_1^{-1}$ , then the quadratic form

$$\mathbf{z}'_i R_i(\gamma_i = 1)^{-1} \mathbf{z}_i = \tilde{\mathbf{z}}_i M_1 M'_1 \tilde{\mathbf{z}}_i = \boldsymbol{\zeta}'_1 \boldsymbol{\zeta}_1$$

where one can solve  $\boldsymbol{\zeta}_1 = M'_1 \tilde{\mathbf{z}}_i$  quickly.

## References

- Bezener, M., Hughes, J. and Jones, G. (2018). Bayesian spatiotemporal modeling using hierarchical spatial priors, with applications to functional magnetic resonance imaging (with discussion), *Bayesian Analysis* **13**(4): 1261–1313.
- Bottolo, L. and Richardson, S. (2010). Evolutionary stochastic search for Bayesian model exploration, *Bayesian Analysis* **5**(3): 583–618.
- Brechmann, E. C. and Czado, C. (2015). COPAR– multivariate time series modeling using the copula autoregressive model, *Applied Stochastic Models in Business and Industry* **31**(4): 495–514.
- Brown, P. J., Vannucci, M. and Fearn, T. (2002). Bayes model averaging with selection of regressors, *Journal of the Royal Statistical Society: Series B* **64**(3): 519–536.
- Christensen, R. (2011). *Plane Answers to Complex Questions*, 4th edn, Springer.
- Chung, Y. and Dunson, D. B. (2009). Nonparametric Bayes conditional distribution modeling with variable selection, *Journal of the American Statistical Association* **104**(488): 1646–1660.
- Clyde, M. and George, E. I. (2004). Model uncertainty, *Statistical Science* **19**(1): 81–94.
- Davis, J. and Goadrich, M. (2006). The relationship between precision-recall and ROC curves, *Proceedings of the 23rd international conference on Machine learning*, ACM, pp. 233–240.
- Eklund, A., Lindquist, M. A. and Villani, M. (2017). A Bayesian heteroscedastic GLM with application to fMRI data with motion spikes, *Neuroimage* **155**: 354–369.
- George, E. and McCulloch, R. (1993). Variable selection via Gibbs sampling, *Journal of the American Statistical Association* **88**: 881–889.
- George, E. and McCulloch, R. (1997). Approaches to Bayesian variable selection, *Statistica Sinica* **7**: 339–374.
- Gneiting, T., Balabdaoui, F. and Raftery, A. E. (2007). Probabilistic forecasts, calibration and sharpness, *Journal of the Royal Statistical Society: Series B (Statistical Methodology)* **69**(2): 243–268.
- Goldsmith, J., Huang, L. and Crainiceanu, C. M. (2014). Smooth scalar-on-image regression via spatial Bayesian variable selection, *Journal of Computational and Graphical Statistics* **23**(1): 46–64.
- Gössl, C., Fahrmeir, L. and Auer, D. (2001). Bayesian modeling of the hemodynamic response function in BOLD fMRI, *Neuroimage* **14**(1): 140–148.
- Gottardo, R. and Raftery, A. (2009). Bayesian robust transformation and variable selection: A unified approach, *Canadian Journal of Statistics* **37**(3): 361–380.
- Grazian, C. and Liseo, B. (2017). Approximate Bayesian inference in semiparametric copula models, *Bayesian Analysis* **12**(4): 991–1016.

- Green, P. J. and Richardson, S. (2002). Hidden markov models and disease mapping, *Journal of the American Statistical Association* **97**(460): 1055–1070.
- Hoffman, M. D. and Gelman, A. (2014). The No-U-Turn sampler: Adaptively setting path lengths in Hamiltonian Monte Carlo, *Journal of Machine Learning Research* **15**: 1351–1381.
- Joe, H. (2005). Asymptotic efficiency of the two-stage estimation method for copula-based models, *Journal of Multivariate Analysis* **94**(2): 401–419.
- Joe, H. (2015). *Dependence Modeling with Copulas*, Chapman & Hall/CRC Monographs on Statistics & Applied Probability, 1st edn, Taylor & Francis.
- Johnson, V. E. and Rossell, D. (2012). Bayesian model selection in high-dimensional settings, *Journal of the American Statistical Association* **107**(498): 649–660.
- Klein, N. and Smith, M. S. (2018). Implicit copulas from Bayesian regularized regression smoothers, *To appear in Bayesian Analysis* .
- Kraus, D. and Czado, C. (2017). D-vine copula based quantile regression, *Computational Statistics & Data Analysis* **110**: 1–18.
- Kundu, S. and Dunson, D. B. (2014). Bayes variable selection in semiparametric linear models, *Journal of the American Statistical Association* **109**(505): 437–447.
- Lee, K.-J., Jones, G. L., Caffo, B. S. and Bassett, S. S. (2014). Spatial Bayesian variable selection models on functional magnetic resonance imaging time-series data, *Bayesian Analysis* **9**(3): 699.
- Li, F. and Zhang, N. R. (2010). Bayesian variable selection in structured high-dimensional covariate spaces with applications in genomics, *Journal of the American statistical association* **105**(491): 1202–1214.
- Liang, F., Paulo, R., Molina, G., Clyde, M. A. and Berger, J. O. (2008). Mixtures of g priors for Bayesian variable selection, *Journal of the American Statistical Association* **103**(481): 410–423.
- Neal, R. M. (2011). MCMC using Hamiltonian dynamics, *in* S. Brooks, A. Gelman, G. Jones and X.-L. Meng (eds), *Handbook of Markov Chain Monte Carlo*, Chapman & Hall / CRC Press, pp. 113–162.
- Nelsen, R. (2006). *An Introduction to Copulas*, 2nd edn, Springer.
- Nott, D. J. and Green, P. J. (2004). Bayesian variable selection and the Swendsen-Wang algorithm, *Journal of Computational and Graphical Statistics* **13**(1): 141–157.
- O’Hara, R. and Sillanpää, M. (2009). A review of Bayesian variable selection methods: What, How, and Which, *Bayesian Analysis* **4**: 85–118.
- Pitt, M., Chan, D. and Kohn, R. (2006). Efficient Bayesian inference for Gaussian copula regression models, *Biometrika* **93**: 537–554.



- Raftery, A. (1996). Hypothesis testing and model selection., in W. R. Gilks, S. Richardson and D. J. Spiegelhalter (eds), *Markov chain Monte Carlo in practice*, Chapman & Hall/CRC, New York/Boca Raton, pp. 163–188.
- Ranciati, S., Galimberti, G. and Soffritti, G. (2019). Bayesian variable selection in linear regression models with non-normal errors, *Statistical Methods & Applications* **28**(2): 323–358.
- Rossell, D. and Rubio, F. J. (2018). Tractable Bayesian variable selection: beyond normality, *Journal of the American Statistical Association* **113**(524): 1742–1758.
- Scott, J. G. and Berger, J. O. (2010). Bayes and empirical-Bayes multiplicity adjustment in the variable-selection problem, *The Annals of Statistics* **38**(5): 2587–2619.
- Sharma, R. and Das, S. (2018). Regularization and variable selection with copula prior, *arXiv:1709.05514v2*.
- Shimazaki, H. and Shinomoto, S. (2010). Kernel bandwidth optimization in spike rate estimation, *Journal of Computational Neuroscience* **29**(1-2): 171–182.
- Sklar, A. (1959). Fonctions de répartition à  $n$  dimensions et leurs marge, *Publications de l'Institut de Statistique de l'Université de Paris* **8**: 229–231.
- Smith, M., Kohn, R. and Mathur, S. K. (2000). Bayesian semiparametric regression: An exposition and application to print advertising data, *Journal of Business Research* **49**: 229–244.
- Smith, M., Ptz, B., Auer, D. and Fahrmeir, L. (2003). Assessing brain activity through spatial Bayesian variable selection, *NeuroImage* **20**(2): 802–815.
- Smith, M. S. (2015). Copula modelling of dependence in multivariate time series, *International Journal of Forecasting* **31**: 815–833.
- Smith, M. S. and Fahrmeir, L. (2007). Spatial Bayesian variable selection with application to functional magnetic resonance imaging, *Journal of the American Statistical Association* **102**(478): 417–431.
- Smith, M. S. and Kohn, R. (1996). Nonparametric regression using Bayesian variable selection, *Journal of Econometrics* **75**(2): 317–343.
- Smith, M. S. and Kohn, R. (2000). Nonparametric seemingly unrelated regression, *Journal of Econometrics* **98**: 257–281.
- Song, P. (2000). Multivariate dispersion models generated from Gaussian copula, *Scandinavian Journal of Statistics* **27**(2): 305–320.
- Wang, L., Yuanyuan Tang, Y., Debajyoti, S., Pati, D. and Stuart Lipsitz, S. (2017). Bayesian variable selection for skewed heteroscedastic response, *Technical report*. arXiv:1602.09100v2.
- Wauthier, F. L. and Jordan, M. I. (2010). Heavy-tailed process priors for selective shrinkage, *Advances in Neural Information Processing Systems*, pp. 2406–2414.

- Wilson, A. G. and Ghahramani, Z. (2010). Copula processes, *Advances in Neural Information Processing Systems*, pp. 2460–2468.
- Yan, Y. and Kottas, A. (2017). A new family of error distributions for Bayesian quantile regression, *Technical report*. arXiv:1701.05666.
- Yu, K., Chen, C., Reed, C. and Dunson, D. (2013). Bayesian variable selection in quantile regression, *Statistics and its interface* **6**: 261–274.
- Zellner, A. (1986). On assessing prior distributions and Bayesian regression analysis with g prior distributions, *in* P. Goel and A. Zellner (eds), *Bayesian Inference and Decision Techniques: Essays in Honour of Bruno de Finetti*, pp. 233–243.

Prior for $g$				
Model	hyper-g	hyper-g/n	Zellner-Siow	$g = 100$
<i>In-sample log-scores</i>				
BVSC	<b>97.022</b>	<b>96.984</b>	<b>96.243</b>	87.794
BVS	90.978	90.875	90.838	<b>89.970</b>
<i>Predictive log-scores</i>				
BVSC	<b>103.569</b>	<b>103.626</b>	<b>103.344</b>	<b>97.603</b>
BVS	99.583	99.423	99.430	95.255

Table 1: Mean logarithmic scores (multiplied by 100) computed from the predictive densities of  $Y$  from the eight regression models fit to the advertising dataset. Results from both the copula (BSVC) and regular (BVS) Bayesian variable selection methods are reported, each using four different priors for  $g$ . Scores are broken down by the in-sample values (first twelve magazine issues) and the out-of-sample period (thirteenth issue).

Variable	BVSC	BVS	BVSC	BVS	BVSC	BVS	BVSC	BVS
	hyper-g	hyper-g	hyper-g/n	hyper-g/n	Zellner-Siow	Zellner-Siow	$g = 100$	$g = 100$
$X_{79}$	1.000	1.000	1.000	1.000	1.000	1.000	1.000	1.000
$X_{54}$	0.999	1.000	1.000	1.000	1.000	1.000	1.000	1.000
$X_{55}$	0.999	1.000	0.998	1.000	1.000	1.000	1.000	1.000
$X_{24}$	0.979	0.144	0.978	0.141	0.990	0.142	0.896	0.223
$X_{241}$	0.976	1.000	0.985	1.000	0.980	1.000	0.505	1.000
$X_{242}$	0.954	0.274	0.963	0.266	0.955	0.258	0.455	0.372
$X_{249}$	0.932	0.182	0.934	0.172	0.910	0.163	0.147	0.285
$X_{48}$	0.926	0.038	0.923	0.033	0.936	0.034	0.157	0.095
$X_{50}$	0.903	0.023	0.897	0.018	0.897	0.019	0.028	0.058
$X_{139}$	0.885	0.103	0.879	0.082	0.885	0.083	0.101	0.124
$X_{110}$	0.813	0.135	0.808	0.130	0.763	0.124	0.416	0.222
$X_{164}$	0.776	0.170	0.782	0.171	0.798	0.159	0.005	0.269
$X_{45}$	0.759	0.169	0.752	0.165	0.678	0.160	0.018	0.233
$X_{109}$	0.756	0.012	0.757	0.011	0.749	0.011	0.147	0.038
$X_{66}$	0.745	0.005	0.741	0.004	0.663	0.004	0.092	0.020
$X_{165}$	0.690	0.125	0.672	0.121	0.564	0.118	0.967	0.183
$X_{78}$	0.669	0.275	0.673	0.284	0.648	0.268	0.002	0.369
$X_{46}$	0.640	0.042	0.640	0.041	0.724	0.039	0.986	0.080
$X_{240}$	0.593	0.021	0.590	0.020	0.534	0.018	0.019	0.057
$X_{123}$	0.590	0.045	0.580	0.043	0.403	0.043	0.000	0.109
$X_{31}$	0.520	0.234	0.510	0.232	0.410	0.232	0.256	0.301
$X_{120}$	0.477	0.200	0.484	0.189	0.548	0.179	0.661	0.263
$X_2$	0.460	0.452	0.478	0.427	0.444	0.401	0.404	0.431
$X_7$	0.447	0.485	0.459	0.480	0.433	0.471	0.282	0.442
$X_3$	0.442	0.386	0.412	0.371	0.402	0.387	0.328	0.390
$X_{247}$	0.439	0.036	0.432	0.034	0.426	0.035	0.282	0.066
$X_6$	0.428	0.474	0.427	0.464	0.451	0.443	0.267	0.407
$X_{67}$	0.414	0.998	0.423	0.998	0.489	0.998	0.056	0.985
$X_{176}$	0.407	0.159	0.420	0.153	0.496	0.151	0.868	0.171
$X_5$	0.401	0.394	0.413	0.470	0.426	0.433	0.311	0.412
$\mathbb{E}(q_\gamma \mathbf{y})$	41.8	21.0	41.1	20.8	35.0	20.9	17.6	25.7
$\text{Var}(q_\gamma \mathbf{y})$	5.2	2.6	5.1	2.6	3.7	2.6	1.8	3.5

Table 2: Marginal posterior probabilities  $\Pr(\gamma_i = 1|X, \mathbf{y})$  in the print advertising example. The first column lists the 30 variables with the highest probabilities when using the BVSC model with the hyper-g prior, which is the best performing model. Also listed are the probabilities for the same variables from the other seven models. The last two rows report the posterior moments for the number of selected variables  $q_\gamma$  for each model.

Prior	hyper-g		hyper-g/n		Zellner-Siow		$g = 100$	
	SBVSC	SBVS	SBVSC	SBVS	SBVSC	SBVS	SBVSC	SBVS
Active	-411.652	-450.717	-411.649	-450.717	-411.648	-450.717	-418.371	-451.082
Inactive	-408.116	-416.480	-408.116	-416.480	-408.116	-416.480	-408.316	-416.532
Overall	-408.172	-416.922	-408.172	-416.922	-408.172	-416.922	-408.420	-416.962

Table 3: Mean logarithmic scores of the MR signal (multiplied by 100) for the eight regression models fit to the fMRI dataset. Results from both the copula (SBVSC) and regular (SBVS) spatial Bayesian variable selection methods are reported, each using four different priors for  $g$ . Results are broken down by active, inactive and all voxels.

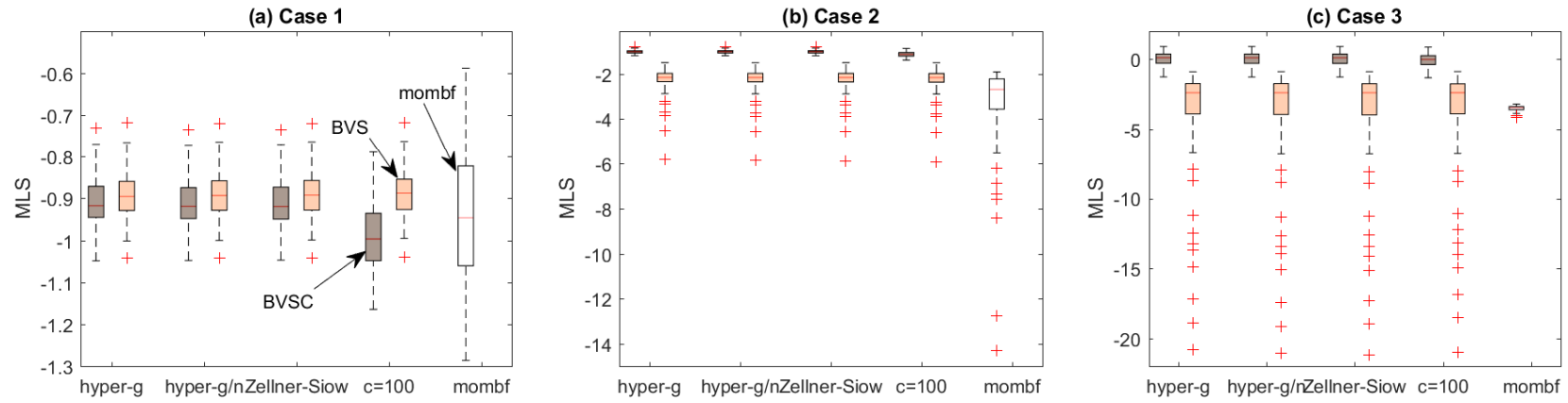


Figure 1: Comparison of the predictive MLS from the simulation study. The three panels provide results for the three cases. Each boxplot is of the 100 values of the MLS from the 100 simulation replicates, where higher values correspond to increased accuracy. In each panel, the first eight boxplots correspond to combinations of the methods BVSC and BVS with the four priors for  $g$ . The last column (white boxplot) corresponds to the mombf/ $N$  method.

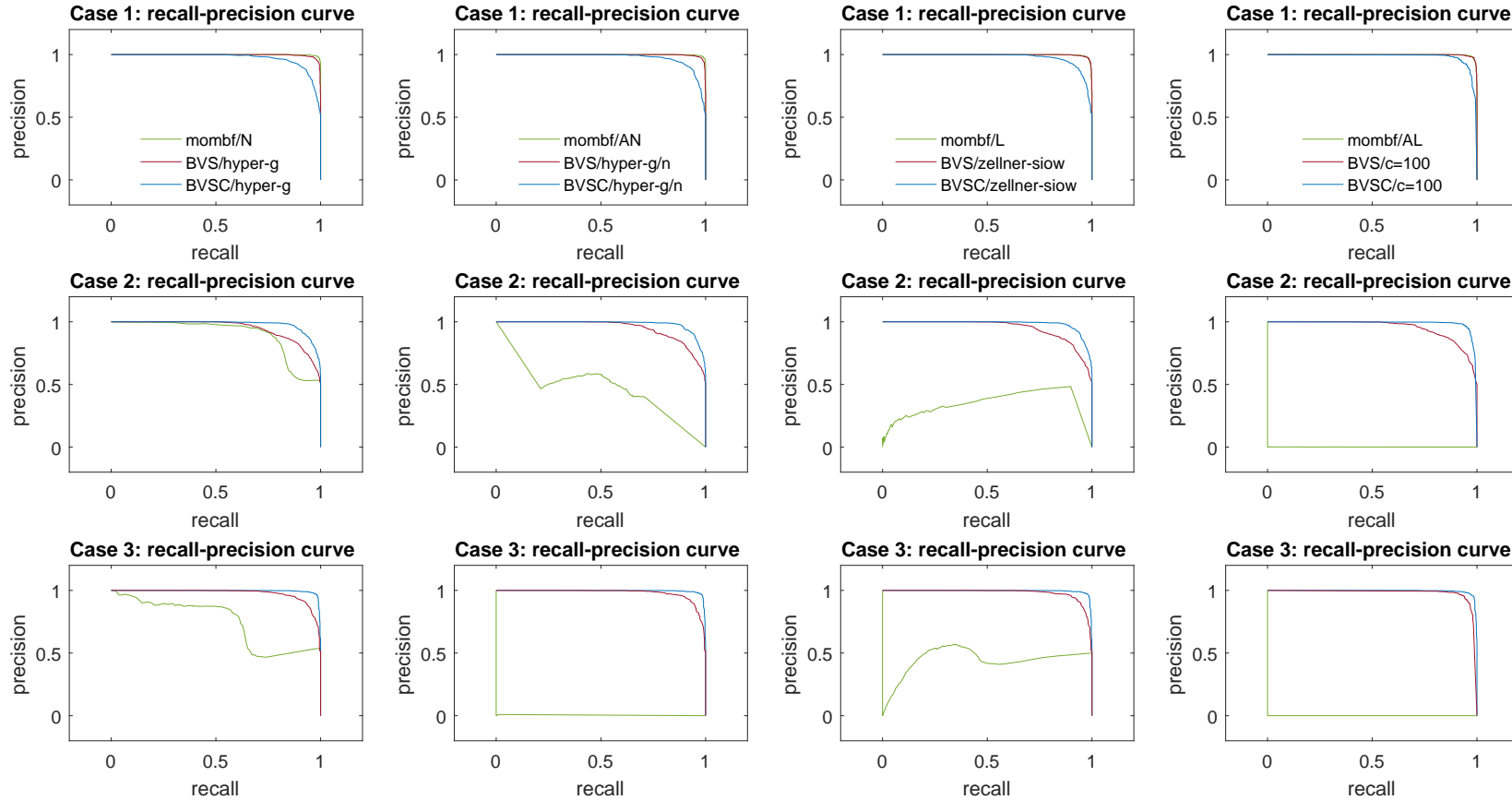


Figure 2: Comparison of the average recall-precision curves from the simulation study for a grid of thresholds in  $(0, 1)$ . The first row (ie. panels a,b,c,d) show results for case 1, the second row (ie. panels e,f,g,h) for case 2, and the third row (ie. panels i,j,k,l) for case 3. Each panel contains curves for the BVSC (blue) and the BVS (red) methods for one specific prior for  $g$ , along with curves from mombf (red) with one distributional assumption from N (normal), AN (asymmetric normal), L (Laplace) and AL (asymmetric Laplace).

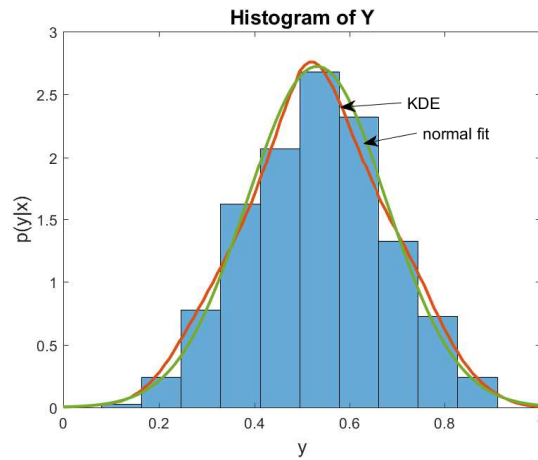


Figure 3: Histogram of the noted score in the print advertising example. Also shown in red is the adaptive kernel density estimate (KDE) as well as a normal fit in green.

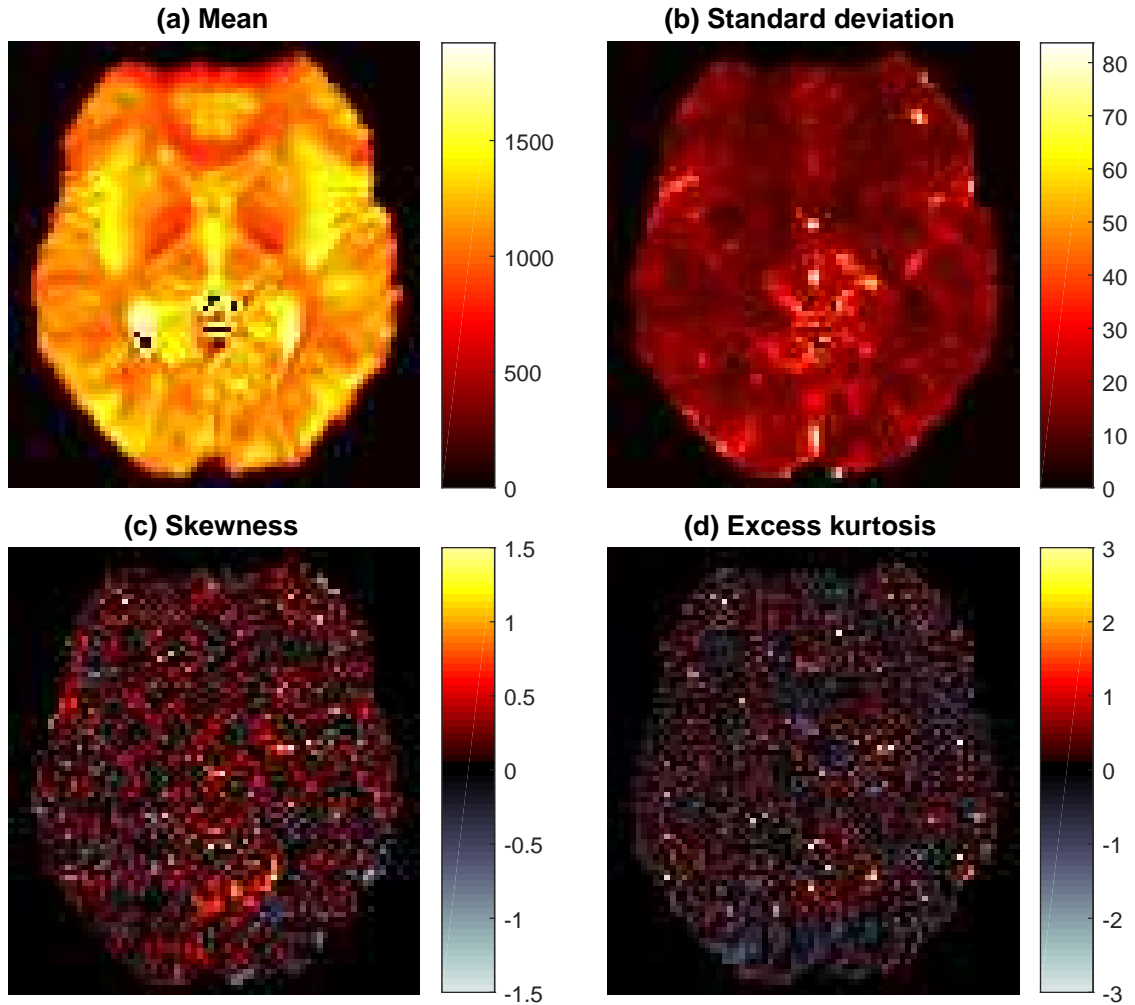


Figure 4: Sample moments of the MR signal at each voxel in the fMRI example. The four panels plot the (a) mean, (b) standard deviation, (c) Pearson skew and (d) excess kurtosis values for each voxel.



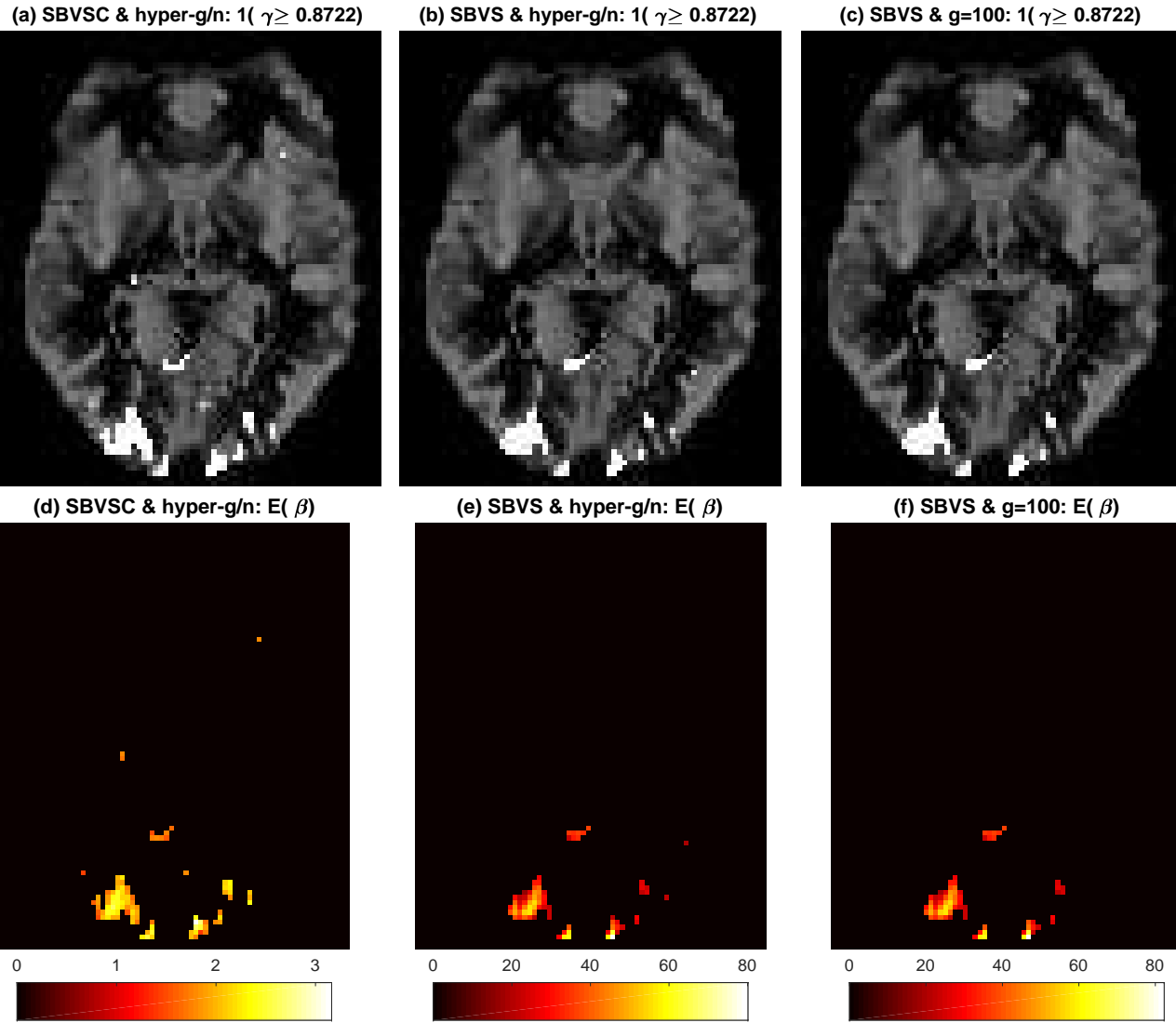


Figure 5: Posterior activation and amplitude maps for the fMRI data from three different estimators. The first row shows the activation maps (where white voxels are those classified as active), and the second shows the mean activation amplitudes. The three different estimators are: (a,d) SBVSC with hyper-g/n prior; (b,e) SBVS with hyper-g/n prior; and, (c,f) SBVS with  $g = 100$  which is the model used in Smith and Fahrmeir (2007).

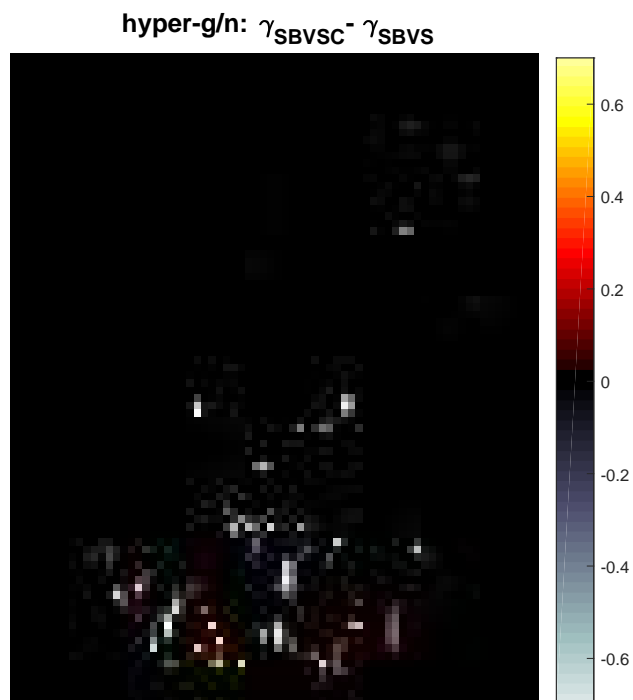


Figure 6: Difference between the activation probabilities of the copula (SBVSC) and Gaussian (SBVS) spatial Bayesian variable selection models for the fMRI data. The difference is SBVSC minus SBVS, and both models employ the same Ising prior for  $\gamma$  and hyper-g/n prior for  $g$ .